

Lick 2.4-m Primary Mirror

Final Test Report

Rayleigh Optical Corporation

September 7, 2007

Table of Contents

1. Figure Quality.
 - 1.1. Test configuration
 - 1.2. Null lens and CGH design and manufacture.
 - 1.3. Test optic error determination.
 - 1.4. Final figure and interferograms.
 - 1.5. Centration of the optical axis.

2. Radius of curvature and conic constant..
 - 2.1. Measurement of the final radius.
 - 2.2. Determination of the conic constant.

3. Cosmetic quality.
 - 3.1. Scratch/dig
 - 3.2. Surface microroughness.

1. Figure Quality.

1.1. Test configuration.

Final figuring and testing of the mirror was performed in ROC's 12-meter test tower with the mirror installed in the telescope cell provided by EOST. A three-element Offner null corrector lens system integrated with a phase-measuring interferometer was positioned at the top of the tower near the mirror's center of curvature. A schematic of the test configuration is depicted in Figure 2 and a schematic of the interferometer/null corrector system is shown in Figure 1.

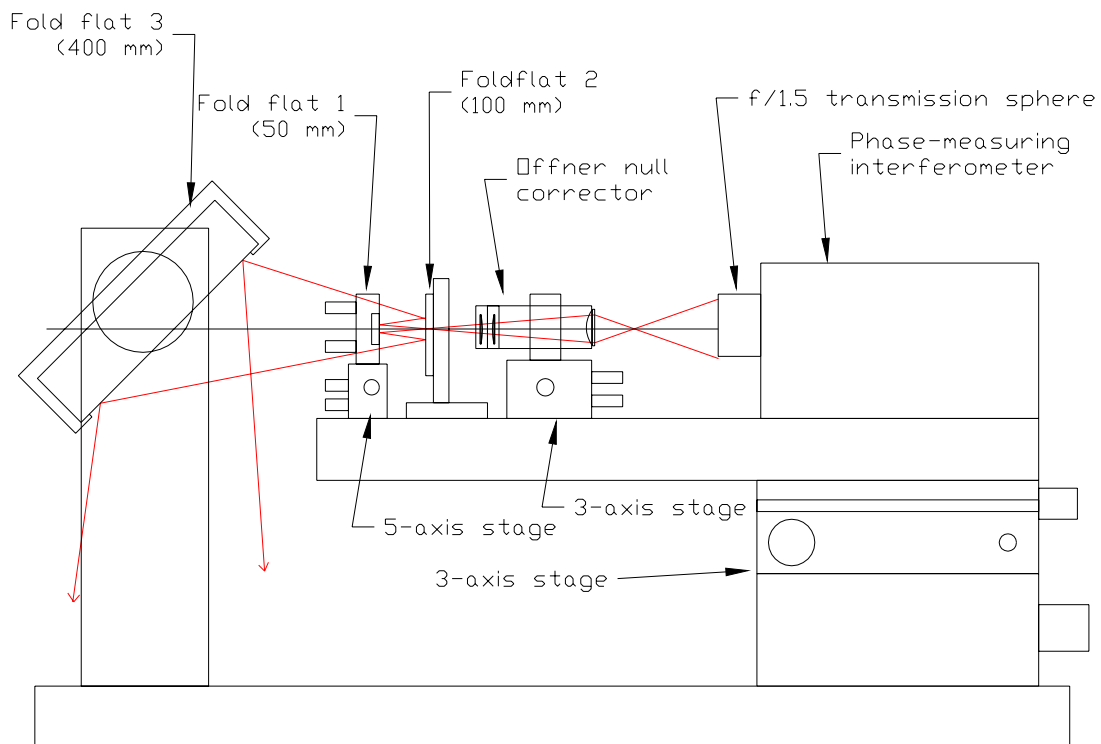


Figure 1a. A side view of the interferometer system to test the mirror using a 3-element Offner null corrector. The beam is folded twice to both align the null corrector to the mirror and to fold the beam downward.

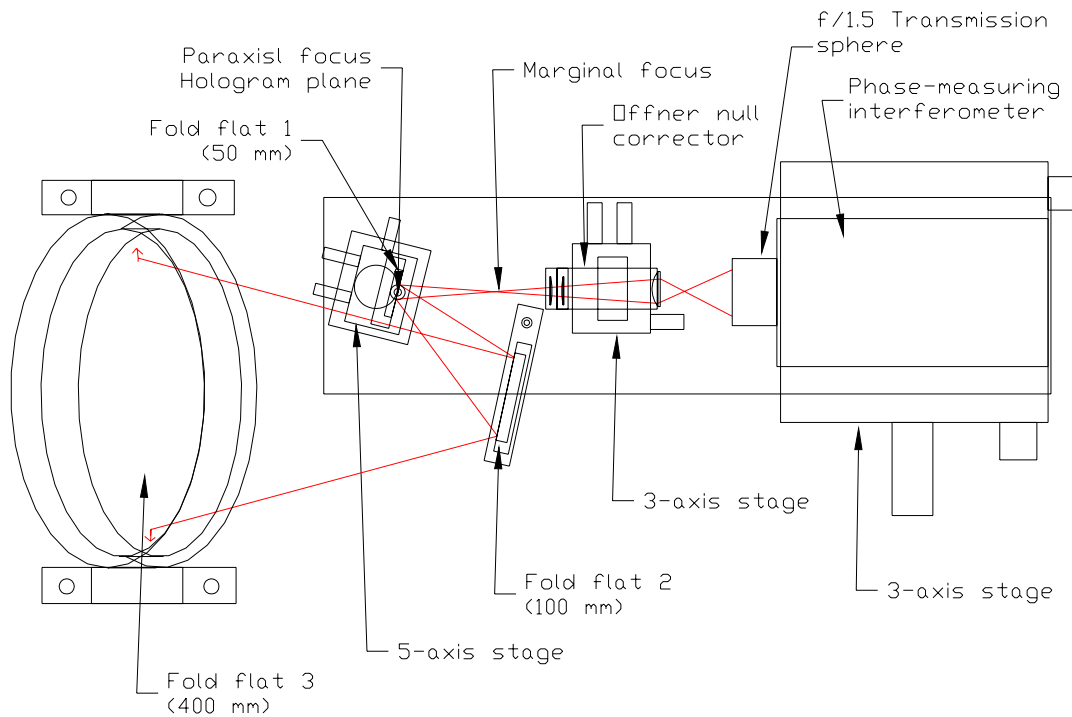


Figure 1b. A top view of the interferometer system shows the direction of the folds and the position of the paraxial focus at the surface of flat 1. This is also the hologram plane where the CGH is designed to be placed to verify the quality of the null corrector.

The interferometer system consists of a 100 mm aperture Fizeau interferometer working at 633 nm with an $f/1.5$ transmission sphere that forms both the transmitted spherical wavefront out to the null lens and the reference wavefront from its spherical exit surface. The spherical wavefront passes through focus and enters the null lens at a focal ratio of $f/1.7$. After passing through the null lens the beam is directed through three fold flats that are used to fold the beam downward to the mirror as well as for alignment. Three flats were required instead of the usual single flat due to the fact that the system required reconfiguring after the move of the mirror to the larger tower from a more suitable smaller tower where the interferometer was initially installed. The telescope mirror cell proved to be too large for the original tower necessitating a somewhat awkward system to get the source point to the correct position at the mirror's center of curvature.

The first fold flat having an aperture of 50 mm is mounted in a gimbale mount that allows the mirror to tip and tilt about the center of the reflecting surface. For the reconfiguration this mount was itself mounted on a rotating base that allows rotation of the assembly about a vertical axis passing through the mirror's surface so the flat can be rotated approximately 20 degrees to fold the beam to the second fold flat. The fold flat is positioned such that the paraxial center of curvature of the mirror and null lens fall on the center of the mirror. This is accomplished as described below in the section on null lens verification. This position allows for the accurate measure of the mirror's radius of curvature by fixing the center of curvature at a physical surface we can measure to.

Because this flat is located at the paraxial center of curvature it is in a location highly suitable for alignment of the null lens's optical axis to the mirror's optical axis. Small tilts of the null lens axis about a point near the center of curvature introduces coma into the wavefront with virtually no tilt. To accurately and remotely align the null lens with the mirror from the control computer's location, the gimbel mount is motorized with small DC actuators and remotely controlled.

A very high quality, 100 mm diameter flat is used for the second fold flat. Its only function is to fold the beam out to the third fold flat, a 400 mm diameter flat mounted such that it folds the beam downward to the mirror.

As shown in Figure 2, the test tower functions not only as a test platform but is also equipped with an integrated polishing machine allowing the mirror to be tested and figured without moving the mirror. Various sorts of polishing tools can be mounted on the polishing arm then the assembly can be swung out of the way for optical testing. The polishing machine's base was upgraded with the support of Lick during the fabrication improving the polishing rate and stability and safety of the machine.

Throughout final figuring and testing the mirror was supported by the telescope cell's 27 axial supports and laterally through the cell's three-armed lateral restraint plate attached to the mirror through three small pads bonded to the rear surface. No other axial or lateral forces were acting on the mirror during testing although four earthquake stops were snugged up against the mirror during polishing runs in the event of a failure of the support system. These were not, in fact, needed since the support system appeared to function extremely well during the fabrication and testing with a high level of stability and repeatability.

At the base of the tower is a 96" diameter turntable onto which the mirror cell is clamped at four locations directly under the cell arms. This turntable is used both in figuring to rotate the mirror under the polishing head, as well as in the optical testing to allow the mirror to be tested at various orientations. Supporting the entire tower, turntable, mirror, and mirror cell are a set of 12 Newport vibration isolation mounts.

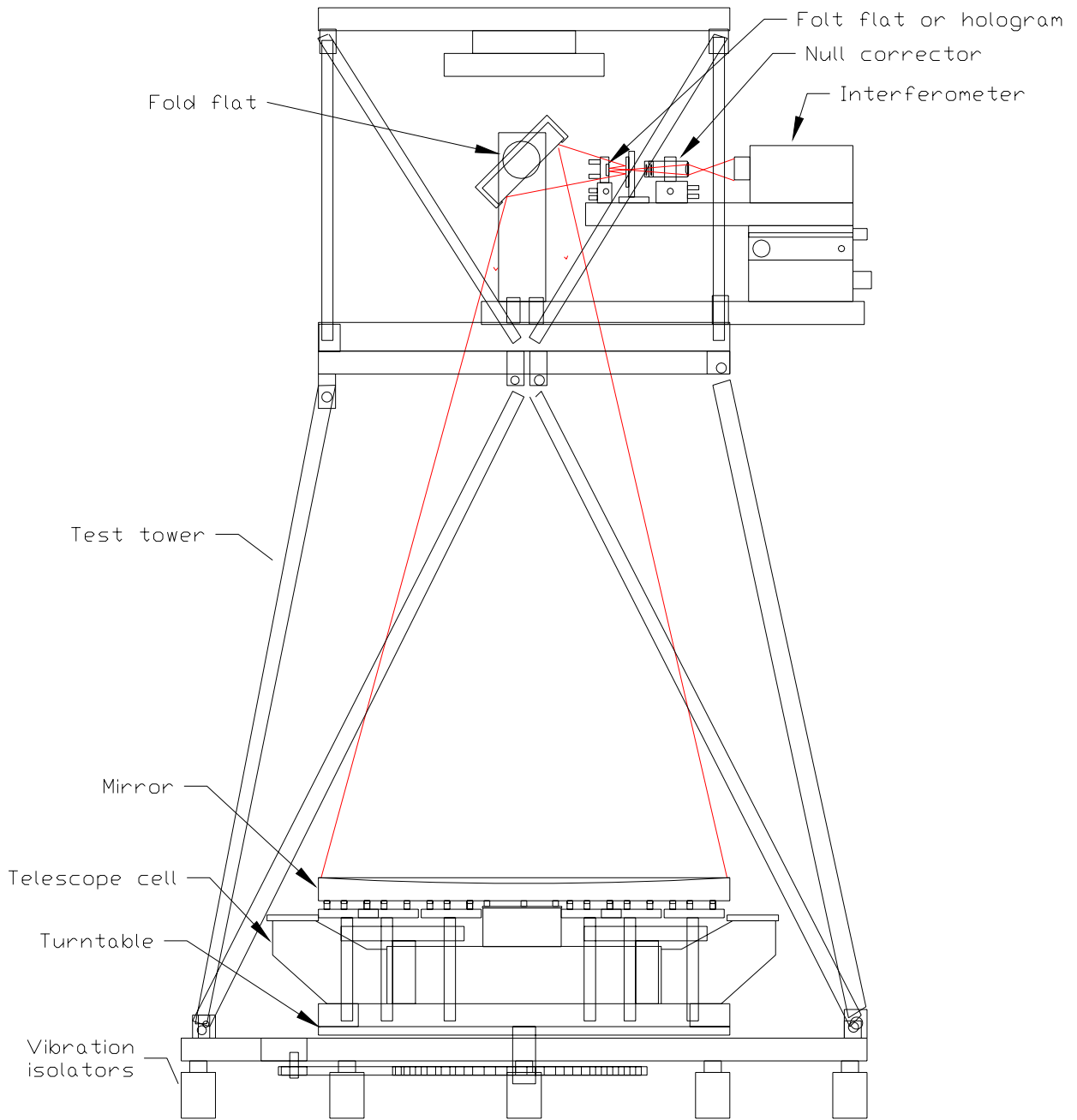
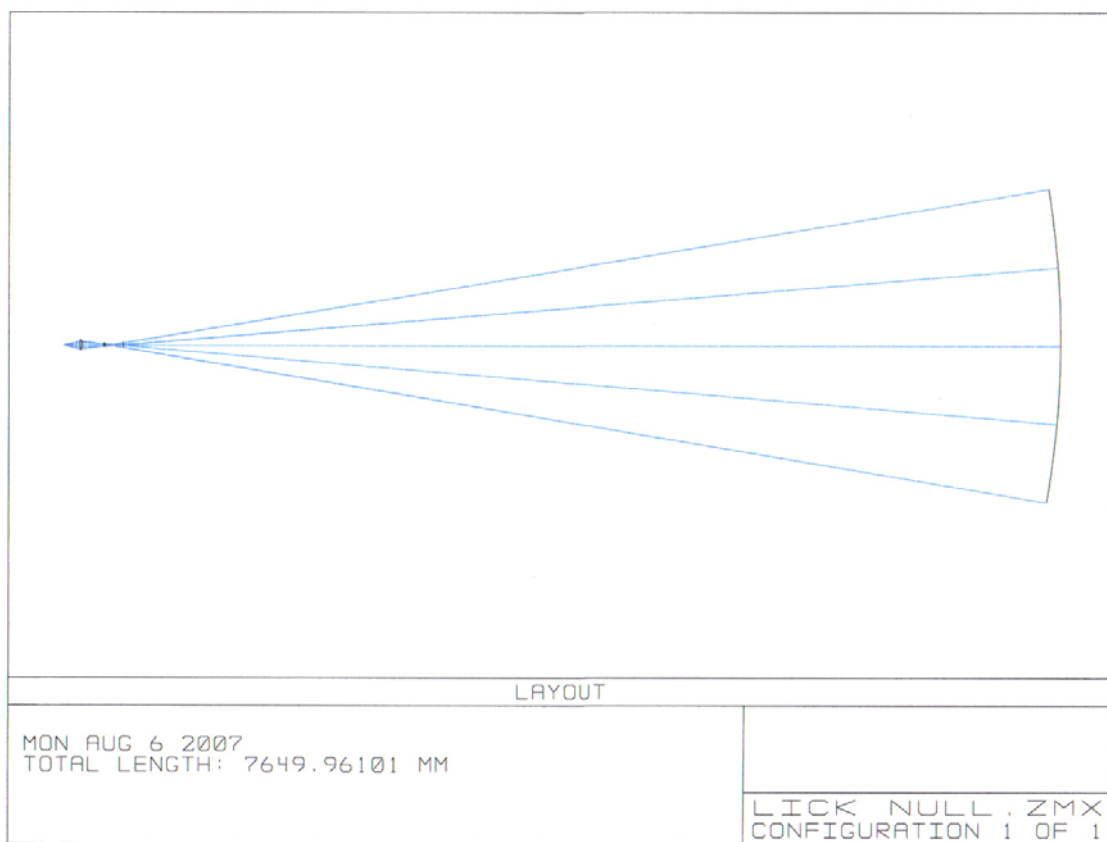


Figure 2. The mirror is tested from its center of curvature with an Offner null corrector nulling the spherical aberration. Final figuring and testing were performed with the mirror installed in its telescope cell.

1.2. Null lens and CGH design and manufacture.

Figure 3 shows the optical layout of the Offner type null corrector used to null the spherical aberration resulting from testing at the mirror's center of curvature. This design is actually the second design and null corrector built and used to test the mirror. The original null lens had only a single field lens but unfortunately due to an unusual interaction of radius of curvature and spherical aberration of the relay lens a badly placed ghost image appeared that was not noticed in the original design before it was constructed. A new design utilizing the existing relay lens was performed but it was found that two lenses would be required to eliminate the ghost reflection. This is the null lens that was used for the majority of the final figuring and all of the testing.



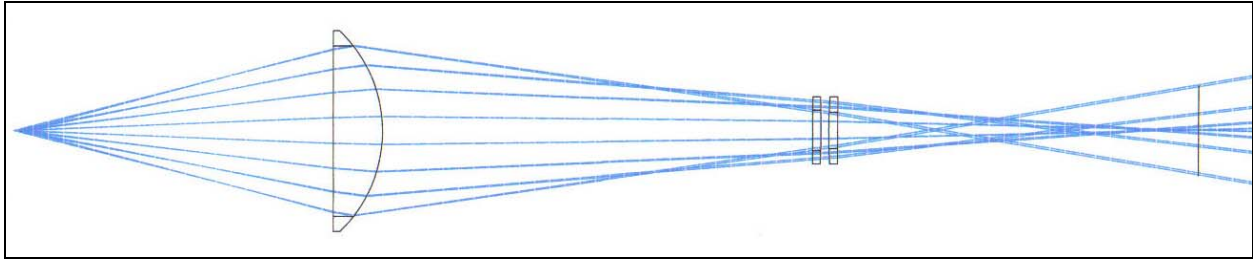


Figure 3. Layout drawings of the null test of the primary mirror (above) and the detail of the null corrector. (below)

Figure 4 contains the surface data summary for the null lens design. The complete design can be found in Appendix A.


```

GENERAL LENS DATA:

Surfaces          :          16
Stop              :           8
System Aperture  : Float By Stop Size = 1200
Glass Catalogs   : SCHOTT
Ray Aiming       : Paraxial Reference, Cache On
  X Pupil shift   :           0
  Y Pupil shift   :           0
  Z Pupil shift   :           0
Apodization      : Uniform, factor = 0.00000E+000
Effective Focal Length : 37.73496 (in air at system temperature and pressure)
Effective Focal Length : 37.73496 (in image space)
Back Focal Length : 154.7869
Total Track      : 7647.153
Image Space F/#  : 0.8810274
Paraxial Working F/# : 1.729532
Working F/#      : 1.978668
Image Space NA   : 0.2777229
Object Space NA  : 0.2682215
Stop Radius      : -1200
Paraxial Image Height : 0
Paraxial Magnification : 0
Entrance Pupil Diameter : 42.83063
Entrance Pupil Position : -44.30476
Exit Pupil Diameter : 42.83063
Exit Pupil Position : 74.10853
Field Type       : Angle in degrees
Maximum Field    : 0
Primary Wave     : 0.6328
Lens Units       : Millimeters
Angular Magnification : 0

Fields           : 1
Field Type: Angle in degrees
#    X-Value      Y-Value      Weight
1    0.000000     0.000000     1.000000

Vignetting Factors
#    VDX          VDY          VCX          VCY          VAN
1    0.000000     0.000000     0.000000     0.000000     0.000000

Wavelengths     : 1
Units: µm
#    Value        Weight
1    0.632800     1.000000

SURFACE DATA SUMMARY:

Surf   Type      Comment      Radius      Thickness    Glass      Diameter    Conic
OBJ STANDARD      RELAY LENS   Infinity    121.221     BK7        61.16655    0
1 STANDARD      RELAY LENS   -52.475     18.77       BK7        61.16655    0
2 STANDARD      KPX630      Infinity    163.5332    BK7        76           0
3 STANDARD      KPX630      -389.04     3.21        BK7        25.4        0
4 STANDARD      KPX630      -389.04     3           BK7        25.4        0
5 STANDARD      KPX621      233.424     3.35        BK7        25.4        0
6 STANDARD      KPX621      Infinity    136.8768    BK7        25.4        0
7 STANDARD      PM          -7200       7200        MIRROR     34.12903    0
STO STANDARD      PM          -7200       -7200       MIRROR     2400        -1
9 STANDARD      PM          Infinity    -136.8768   MIRROR     32.53763    0
10 STANDARD      PM          Infinity    -3.35       BK7        13.1033     0
11 STANDARD      PM          233.424     -3          BK7        13.81255    0
12 STANDARD      PM          -389.04     -3.21       BK7        14.76948    0
13 STANDARD      PM          Infinity    -163.5332   BK7        15.34919    0
14 STANDARD      PM          -52.475     -18.77      BK7        64.46038    0
15 STANDARD      PM          Infinity    -118.4133   BK7        61.85348    0
IMA STANDARD      PM          Infinity    0.001171664 0
  
```

Figure 4. The lens surface summary of the null corrector design.

Figure 5 is a plot of the residual design error with this 3-element design. There is a 6.8 nm rms error from the design that is calibrated out with the CGH test of the lens as described below.

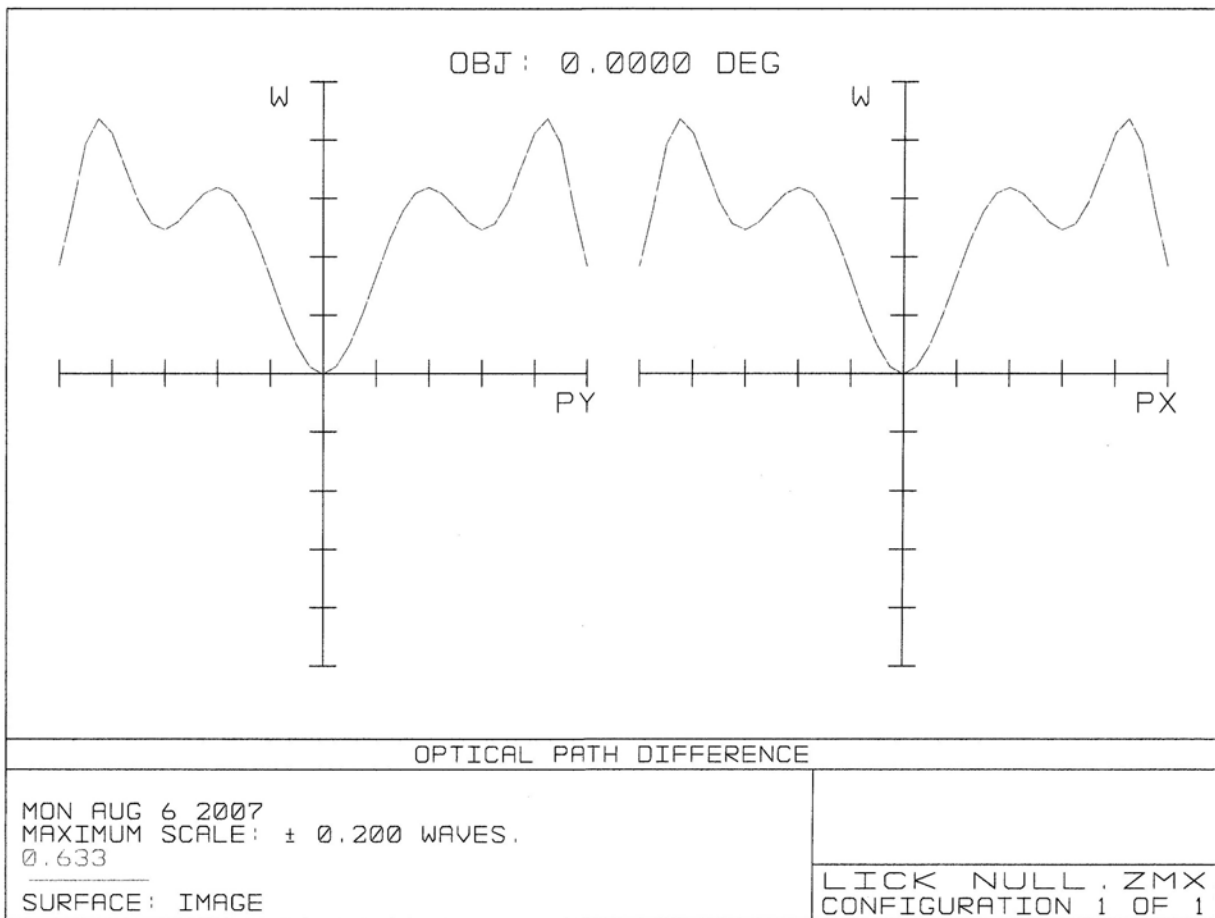


Figure 5. A residual radial error plot of the null corrector's wavefront. This error corresponds to 6.8 nm rms of error in a mirror surface measurement. This error is calibrated out of the test with a CGH test.

The lenses were fabricated to very strict tolerances conforming to ROC's procedures for the fabrication of high quality null optics. As-manufactured radii and lens thicknesses were used in the final design to determine the best spacings for the elements, and these are what are shown above in the final design. The lenses were mounted in precision cells to precise spacing and

centering requirements and the complete corrector was mounted on a 3-axis stage at the proper spacing from the source point.

A very powerful method of verifying the quality of this type of null corrector is through the use of a computer generated hologram or CGH. In this method, a hologram is made of the primary mirror such that when the CGH is placed at the paraxial focus of the null corrector it appears to the interferometer to be looking at a perfect primary mirror having the correct radius of curvature and conic constant. The alignment of the hologram to the null lens is exactly the same as though the hologram were the primary mirror. Since no auxiliary optics are used in the test any errors measured in the test are from the null corrector with a very small contribution from the hologram itself. This allows an accurate measure of the residual errors in the null corrector that can be stored and subtracted from the test of the mirror itself when the hologram is removed and replaced with the fold flat sending the beam to the primary mirror.

The CGH for the primary mirror consists of a 35 mm diameter pattern of chrome rings written onto a flat substrate. The CGH is identified in this report as ROC-PM2. The hologram was designed using software that calculates ring positions based on the geometry of the wavefront reflected from the ideal mirror. The parameters for the CGH are shown in Table 1 and the design is shown in Figure 6.

CGH type	Chrome on glass
Filename with parameters	ROC-PM2.H
Duty Cycle	50%
Number of rings	7082
Outside ring radius	17.730 mm
Outside ring width	0.94 μm
Substrate flatness	< 0.006 wave rms over clear aperture
Pattern scale error	< 0.5 $\mu\text{m}/\text{radius}$
Pattern distortion	< 0.040 μm rms

Table 1. The design parameters for the null corrector CGH.

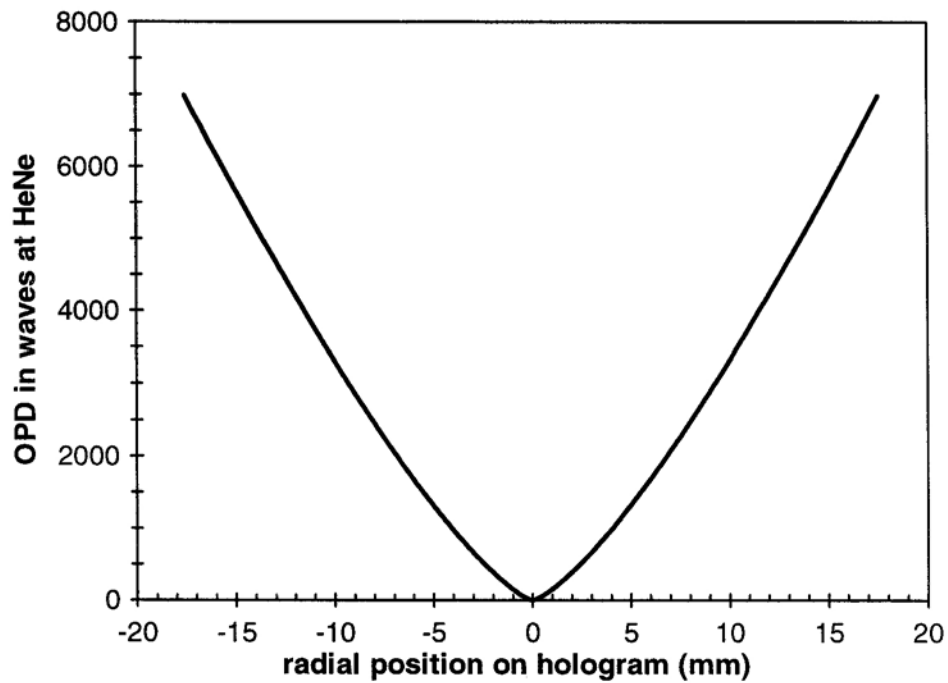


Figure 6a. Design of Lick hologram CGH ROC-PM2. The rings are placed so that each ring corresponds to exactly one wave of optical path difference (OPD).

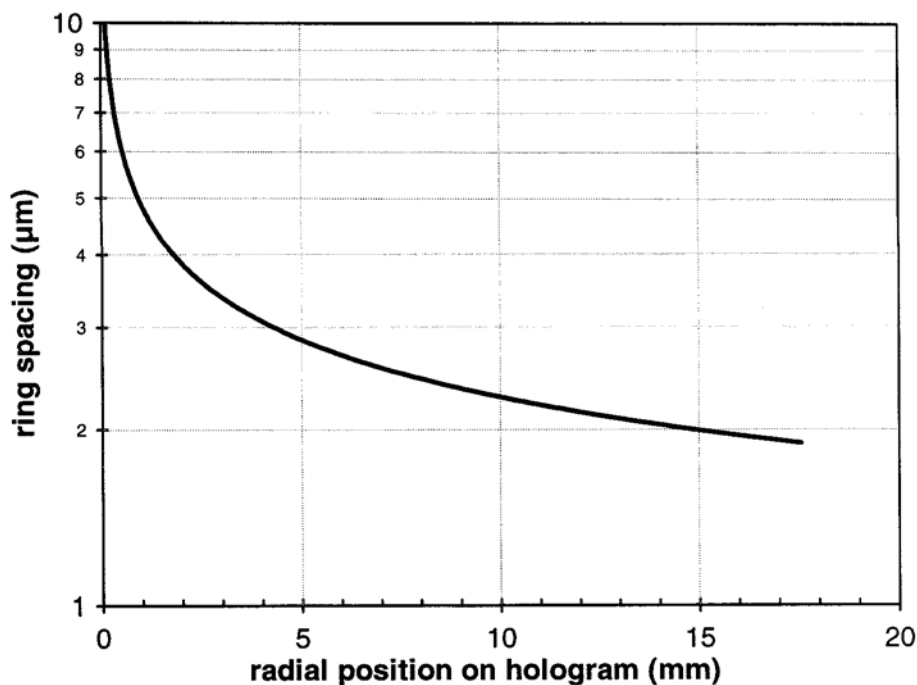


Figure 6b. This plot shows the center-to-center ring spacing across the radial position on the CGH.

What allows for the high accuracy of the CGH measurement is the very high accuracy of the machine used to write the hologram and the methods used to verify that quality. A summary of an analysis of the accuracy of this CGH is given in Table 2. It is based on the measurements provided by the IAE. The complete report can be found in the Appendix along with a description of the methods used to verify the quality of the hologram. Included there are some references to other papers on this method of testing and manufacture of high-precision CGH's.

Error term	dK (ppm)	in waves	
		SA p-v	figure rms
hologram distortion (μm scale)	0.5	60	0.016
hologram distortion (μm rms)	0.04		0.0070
substrate figure (rms waves)	0.006		0.0060
chrome thickness variation (nm rms)	2		0.0032
root sum squared	60	0.016	0.0098
equivalent nm rms		3.1	6.2

Table 2. Summary of the accuracy of the CGH used to test the null corrector.

The CGH is designed to be placed at the paraxial focus of the null corrector whose position relative to the last surface of the corrector is given in the design. As previously described, fold flat 1 is placed at this position such that its surface lies at the paraxial focus as well. To accurately determine this location the fold flat is simply replaced with the CGH such that the CGH's surface is in the same location. It now appears to the interferometer to be looking at a perfect primary mirror. To average out any small asymmetric errors in the hologram we tested the null corrector at 8 different rotations of the hologram 45 degrees apart. The result of this measurement is shown in Figure 7a with the 36 term fit Zernike coefficients shown in 7b. The software used throughout the testing is Intellwave from ESD, Inc. In the case of the CGH measurements vibration is small enough that we could use the phase-stepping algorithm resulting in very smooth, low noise measurements. The values in all of the measurements shown in all maps in this report are **surface** residual values, **not wavefront**. This is simply what opticians prefer to use in fabricating and testing the mirror. All surface residuals are in nanometers. We have used a gray-scale palette for this report as it seems to show the surface features most clearly in this format.

The mask that is used is determined in two ways. The primary mirror itself defines the outer diameter mask. Prior to final CGH testing of the null corrector, the mirror was tested and the same outer diameter mask is then used in all CGH testing. This assures that the errors are scaled properly for subtraction. The inner mask for the CGH test was required to be slightly larger than that of the mirror test due to the very bright central portion of the CGH test resulting from all of the other diffraction orders that pass through the imaging aperture stop.


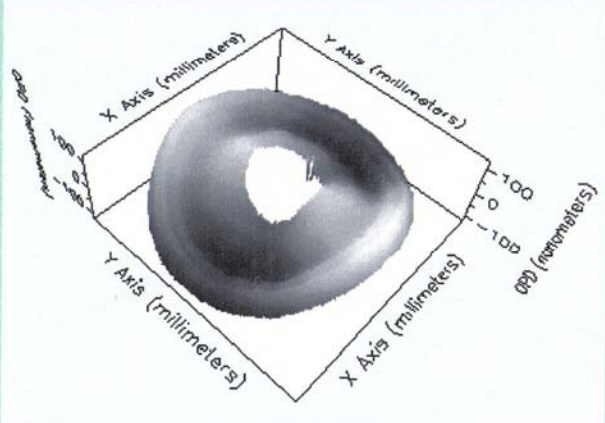
FILE: NULLCALAVG	IntelliWave Report Sheet				
Lick 2.4 m Primary Null Lens	CGH test 8 rotation average				
Surface Map	Surface Map				
					
Data	OPD Statistics:	Value	Min	Max	QC (nanometer)
Wavelength.....0.6328	PV.....	141.3771	0.0000	0.0000	-
Waves/fringe.....0.5000	Peak.....	76.5397	0.0000	0.0000	-
Image Size.....[640, 480]	Center.....	5.8512	0.0000	0.0000	-
Data Aperture: Pos[326, 240] Size[384, 384]	Valley.....	-64.8374	0.0000	0.0000	-
Area Aperture: Pos[320, 240] Size[640, 480]	Average.....	0.0000	0.0000	0.0000	-
Analysis Aper: Pos[326, 240] Size[384, 384]	RMS.....	36.0338	0.0000	0.0000	-
Acquire	#Points.....	103466	0	0	-
#Interferograms: 5	Strehl.....	0.8798	0.0000	0.0000	-
Microns/Volt....1.898402					
Date.....Thu Oct 12 22:30:04 2006					
Unwrapping	RMS Fit:	Value	Min	Max	QC (nanometers)
Name.....[5B,M,MDA]	1	36.0494	0.0000	0.0000	-
Mod. Back.....0.4212	2	19.1732	0.0000	0.0000	-
Date.....Thu Oct 12 22:30:07 2006	3	13.9284	0.0000	0.0000	-
Aberrations	4	7.1408	0.0000	0.0000	-
Name.....UofA	5	4.9000	0.0000	0.0000	-

Figure 7a. The average phase map of 8 rotations of the CGH in the test of the null corrector. Tilt, focus, and coma have been subtracted.

Aber>UofA : Value	Min	Max	QC (nanometers)
1) Piston:	-0.7546	0.0000	0.0000 -
2) X Tilt:	0.1160	0.0000	0.0000 Removed
3) Y Tilt:	-0.8117	0.0000	0.0000 Removed
4) Focus:	1.9583	0.0000	0.0000 Removed
5) X Astig:	-70.3179	0.0000	0.0000 -
6) Y Astig:	8.9547	0.0000	0.0000 -
7) X Coma:	-1.1624	0.0000	0.0000 Removed
8) Y Coma:	2.4752	0.0000	0.0000 Removed
9) Spherical:	6.4417	0.0000	0.0000 -
10) X Trefoil:	3.1636	0.0000	0.0000 -
11) Y Trefoil.:	-12.8410	0.0000	0.0000 -
12) X Astig:	29.6251	0.0000	0.0000 -
13) Y Astig:	-9.3095	0.0000	0.0000 -
14) X Coma:	14.2382	0.0000	0.0000 -
15) Y Coma:	-13.5823	0.0000	0.0000 -
16) Spherical:	-5.4947	0.0000	0.0000 -
17) X Tetrafoil:	7.9872	0.0000	0.0000 -
18) Y Tetrafoil:	-4.4258	0.0000	0.0000 -
19) X Trefoil:	-1.8079	0.0000	0.0000 -
20) Y Trefoil:	13.3549	0.0000	0.0000 -
21) X Astig:	-11.3972	0.0000	0.0000 -
22) Y Astig:	1.3129	0.0000	0.0000 -
23) X Coma:	4.2782	0.0000	0.0000 -
24) Y Coma:	-2.0855	0.0000	0.0000 -
25) Spherical:	-35.2265	0.0000	0.0000 -
26) X Pentafoil:	-1.1166	0.0000	0.0000 -
27) Y Pentafoil:	0.1174	0.0000	0.0000 -
28) X Tetrafoil:	-5.5862	0.0000	0.0000 -
29) Y Tetrafoil:	6.3248	0.0000	0.0000 -
30) X Trefoil:	-0.2270	0.0000	0.0000 -
31) Y Trefoil:	-5.3244	0.0000	0.0000 -
32) X Astig:	11.2553	0.0000	0.0000 -
33) Y Astig:	-1.3829	0.0000	0.0000 -
34) X Coma:	0.2460	0.0000	0.0000 -
35) Y Coma:	-1.1075	0.0000	0.0000 -
36) Spherical:	12.2570	0.0000	0.0000 -

Figure 7b. The Zernike coefficients of the CGH test for the standard set (UofA) of Zernike polynomials.

The raw phase data is fit to a high order set of Zernike polynomials consisting of 205 terms that will accurately reproduce the phase data but will also allow the separation of the rotationally symmetric terms from the asymmetric terms. This is required since the rotationally symmetric errors are what need to be determined from the CGH test that will be subtracted from the measurement of the mirror. Asymmetric errors are introduced into the wavefront not only from the null corrector but also from the three fold flats and interferometer reference as well. To measure the asymmetric errors we measure the mirror over a set of rotations that when averaged allow us to determine the asymmetric errors that do not rotate that are subtracted from the test. The symmetric errors cannot be determined by rotations necessitating this CGH test. Figure 8a shows the result of this high order fit and it should be compared to Figure 7a. Here, the central mask is that determined by the test of the mirror. The first 50 terms of the fit are given in Figure 8b and the full set of the final 205 coefficients determined from both this test and the rotation tests are given in the Appendix.

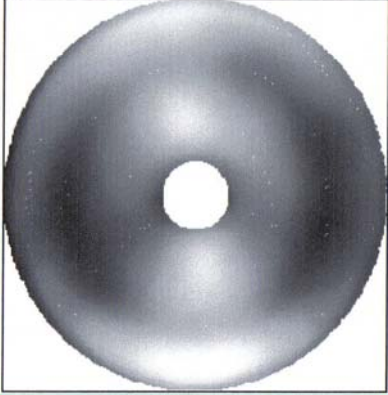
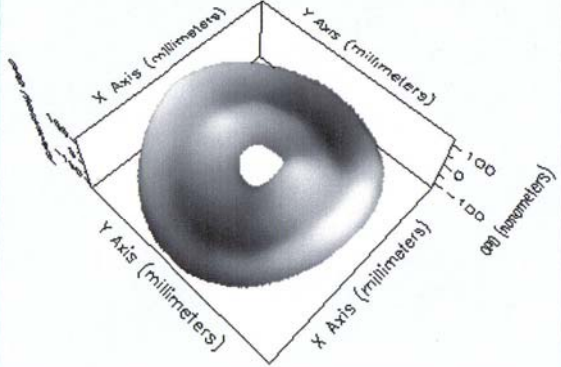
FILE: LICKNULL Lick 2.4 m Primary Null Lens	IntelliWave Report Sheet CGH test High order Zernike fit																																																																																																						
Surface Map	Surface Map																																																																																																						
																																																																																																							
<table border="1"> <thead> <tr> <th>Data</th> <th>OPD Statistics:</th> <th>Value</th> <th>Min</th> <th>Max</th> <th>QC (nanometer)</th> </tr> </thead> <tbody> <tr> <td>Wavelength.....0.6328</td> <td>PV.....</td> <td>140.4482</td> <td>0.0000</td> <td>0.0000</td> <td>-</td> </tr> <tr> <td>Waves/fringe.....-1.0000</td> <td>Peak.....</td> <td>76.4800</td> <td>0.0000</td> <td>0.0000</td> <td>-</td> </tr> <tr> <td>Image Size.....[640, 480]</td> <td>Center.....</td> <td>6.2559</td> <td>0.0000</td> <td>0.0000</td> <td>-</td> </tr> <tr> <td>Data Aperture: Pos[326, 240] Size[384, 384]</td> <td>Valley.....</td> <td>-63.9683</td> <td>0.0000</td> <td>0.0000</td> <td>-</td> </tr> <tr> <td>Area Aperture: Pos[326, 240] Size[384, 384]</td> <td>Average.....</td> <td>-0.0000</td> <td>0.0000</td> <td>0.0000</td> <td>-</td> </tr> <tr> <td>Analysis Aper: Pos[326, 240] Size[384, 384]</td> <td>RMS.....</td> <td>35.3677</td> <td>0.0000</td> <td>0.0000</td> <td>-</td> </tr> <tr> <td>Acquire</td> <td>#Points.....</td> <td>109690</td> <td>0</td> <td>0</td> <td>-</td> </tr> <tr> <td>#Interferograms: 5</td> <td>Strehl.....</td> <td>0.8840</td> <td>0.0000</td> <td>0.0000</td> <td>-</td> </tr> <tr> <td>Microns/Volt....1.898402</td> <td></td> <td></td> <td></td> <td></td> <td></td> </tr> <tr> <td>Date.....Thu Oct 12 22:30:04 2006</td> <td></td> <td></td> <td></td> <td></td> <td></td> </tr> <tr> <td>Unwrapping</td> <td>RMS Fit:</td> <td>Value</td> <td>Min</td> <td>Max</td> <td>QC (nanometers)</td> </tr> <tr> <td>Name.....[5B,M,MDA]</td> <td>1</td> <td>35.9358</td> <td>0.0000</td> <td>0.0000</td> <td>-</td> </tr> <tr> <td>Mod. Back.....0.4212</td> <td>2</td> <td>21.0870</td> <td>0.0000</td> <td>0.0000</td> <td>-</td> </tr> <tr> <td>Date.....Wed Apr 11 22:41:07 2007</td> <td>3</td> <td>20.5513</td> <td>0.0000</td> <td>0.0000</td> <td>-</td> </tr> <tr> <td>Aberrations</td> <td>4</td> <td>17.6811</td> <td>0.0000</td> <td>0.0000</td> <td>-</td> </tr> <tr> <td>Name.....Perkin-Elmer</td> <td>5</td> <td>16.3521</td> <td>0.0000</td> <td>0.0000</td> <td>-</td> </tr> </tbody> </table>	Data	OPD Statistics:	Value	Min	Max	QC (nanometer)	Wavelength.....0.6328	PV.....	140.4482	0.0000	0.0000	-	Waves/fringe.....-1.0000	Peak.....	76.4800	0.0000	0.0000	-	Image Size.....[640, 480]	Center.....	6.2559	0.0000	0.0000	-	Data Aperture: Pos[326, 240] Size[384, 384]	Valley.....	-63.9683	0.0000	0.0000	-	Area Aperture: Pos[326, 240] Size[384, 384]	Average.....	-0.0000	0.0000	0.0000	-	Analysis Aper: Pos[326, 240] Size[384, 384]	RMS.....	35.3677	0.0000	0.0000	-	Acquire	#Points.....	109690	0	0	-	#Interferograms: 5	Strehl.....	0.8840	0.0000	0.0000	-	Microns/Volt....1.898402						Date.....Thu Oct 12 22:30:04 2006						Unwrapping	RMS Fit:	Value	Min	Max	QC (nanometers)	Name.....[5B,M,MDA]	1	35.9358	0.0000	0.0000	-	Mod. Back.....0.4212	2	21.0870	0.0000	0.0000	-	Date.....Wed Apr 11 22:41:07 2007	3	20.5513	0.0000	0.0000	-	Aberrations	4	17.6811	0.0000	0.0000	-	Name.....Perkin-Elmer	5	16.3521	0.0000	0.0000	-	
Data	OPD Statistics:	Value	Min	Max	QC (nanometer)																																																																																																		
Wavelength.....0.6328	PV.....	140.4482	0.0000	0.0000	-																																																																																																		
Waves/fringe.....-1.0000	Peak.....	76.4800	0.0000	0.0000	-																																																																																																		
Image Size.....[640, 480]	Center.....	6.2559	0.0000	0.0000	-																																																																																																		
Data Aperture: Pos[326, 240] Size[384, 384]	Valley.....	-63.9683	0.0000	0.0000	-																																																																																																		
Area Aperture: Pos[326, 240] Size[384, 384]	Average.....	-0.0000	0.0000	0.0000	-																																																																																																		
Analysis Aper: Pos[326, 240] Size[384, 384]	RMS.....	35.3677	0.0000	0.0000	-																																																																																																		
Acquire	#Points.....	109690	0	0	-																																																																																																		
#Interferograms: 5	Strehl.....	0.8840	0.0000	0.0000	-																																																																																																		
Microns/Volt....1.898402																																																																																																							
Date.....Thu Oct 12 22:30:04 2006																																																																																																							
Unwrapping	RMS Fit:	Value	Min	Max	QC (nanometers)																																																																																																		
Name.....[5B,M,MDA]	1	35.9358	0.0000	0.0000	-																																																																																																		
Mod. Back.....0.4212	2	21.0870	0.0000	0.0000	-																																																																																																		
Date.....Wed Apr 11 22:41:07 2007	3	20.5513	0.0000	0.0000	-																																																																																																		
Aberrations	4	17.6811	0.0000	0.0000	-																																																																																																		
Name.....Perkin-Elmer	5	16.3521	0.0000	0.0000	-																																																																																																		

Figure 8a. A map of the CGH test of the null corrector based on a 205 term Zernike fit to the data shown in Figure 7a.

Engineering Synthesis Design Inc. &

	1				2			
23	Aperture Type...inscribed				6	15.8190	0.0000	0.0000 -
24	Removed.....				7	15.6706	0.0000	0.0000 -
25					8	7.3309	0.0000	0.0000 -
26					9	7.2262	0.0000	0.0000 -
27	Aber>Perkin: Value	Min	Max	QC (nanometers)	10	4.1345	0.0000	0.0000 -
28	1) Piston:	-1.4523	0.0000	0.0000 -	11	3.9547	0.0000	0.0000 -
29	2) Tilt:	0.1266	0.0000	0.0000 -	12	3.3048	0.0000	0.0000 -
30	3) Tilt:	-0.6961	0.0000	0.0000 -	13	3.0735	0.0000	0.0000 -
31	4) Focus:	3.8601	0.0000	0.0000 -	14	2.5713	0.0000	0.0000 -
32	5) Astig:	-70.4939	0.0000	0.0000 -	15	2.4569	0.0000	0.0000 -
33	6) Astig:	8.9858	0.0000	0.0000 -	16	1.8598	0.0000	0.0000 -
34	7) Coma:	-1.1390	0.0000	0.0000 -	17	1.7431	0.0000	0.0000 -
35	8) Coma:	1.7718	0.0000	0.0000 -	18	0.0000	0.0000	0.0000 -
36	9) Coma:	3.1640	0.0000	0.0000 -				
37	10) Coma:	-12.7826	0.0000	0.0000 -				
38	11) Spherical:	3.4804	0.0000	0.0000 -				
39	12) Astig:	29.9947	0.0000	0.0000 -				
40	13) Astig:	-9.3654	0.0000	0.0000 -				
41	14) Astig:	8.1631	0.0000	0.0000 -				
42	15) Astig:	-4.4296	0.0000	0.0000 -				
43	16) Coma:	14.2380	0.0000	0.0000 -				
44	17) Coma:	-12.4029	0.0000	0.0000 -				
45	18) Coma:	-1.7718	0.0000	0.0000 -				
46	19) Coma:	13.5419	0.0000	0.0000 -				
47	20) Coma:	-1.1390	0.0000	0.0000 -				
48	21) Coma:	-0.0000	0.0000	0.0000 -				
49	22) Spherical:	-1.2656	0.0000	0.0000 -				
50	23) Astig:	-12.7193	0.0000	0.0000 -				
51	24) Astig:	1.6453	0.0000	0.0000 -				
52	25) Astig:	-5.4421	0.0000	0.0000 -				
53	26) Astig:	6.3280	0.0000	0.0000 -				
54	27) Astig:	0.9492	0.0000	0.0000 -				
55	28) Astig:	1.4554	0.0000	0.0000 -				
56	29) Coma:	4.2398	0.0000	0.0000 -				
57	30) Coma:	-4.1132	0.0000	0.0000 -				
58	31) Coma:	-0.3797	0.0000	0.0000 -				
59	32) Coma:	-5.5054	0.0000	0.0000 -				
60	33) Coma:	1.0758	0.0000	0.0000 -				
61	34) Coma:	-1.0758	0.0000	0.0000 -				
62	35) Coma:	2.5312	0.0000	0.0000 -				
63	36) Coma:	0.7594	0.0000	0.0000 -				
64	37) Spherical:	-40.1195	0.0000	0.0000 -				

Figure 8b. The first 50 coefficients of the 205 term fit.

From the data shown in Figure 8 we only want to know from this test the symmetric terms and this is what is shown in Figure 9. All of the asymmetric terms have been subtracted leaving the symmetric errors that will become the symmetric portion of the test optic error. The first 50 terms of this map are shown in Figure 9b. There is a very close correspondence of this map to the design residual error shown in Figure 5 indicating a well fabricated null lens.

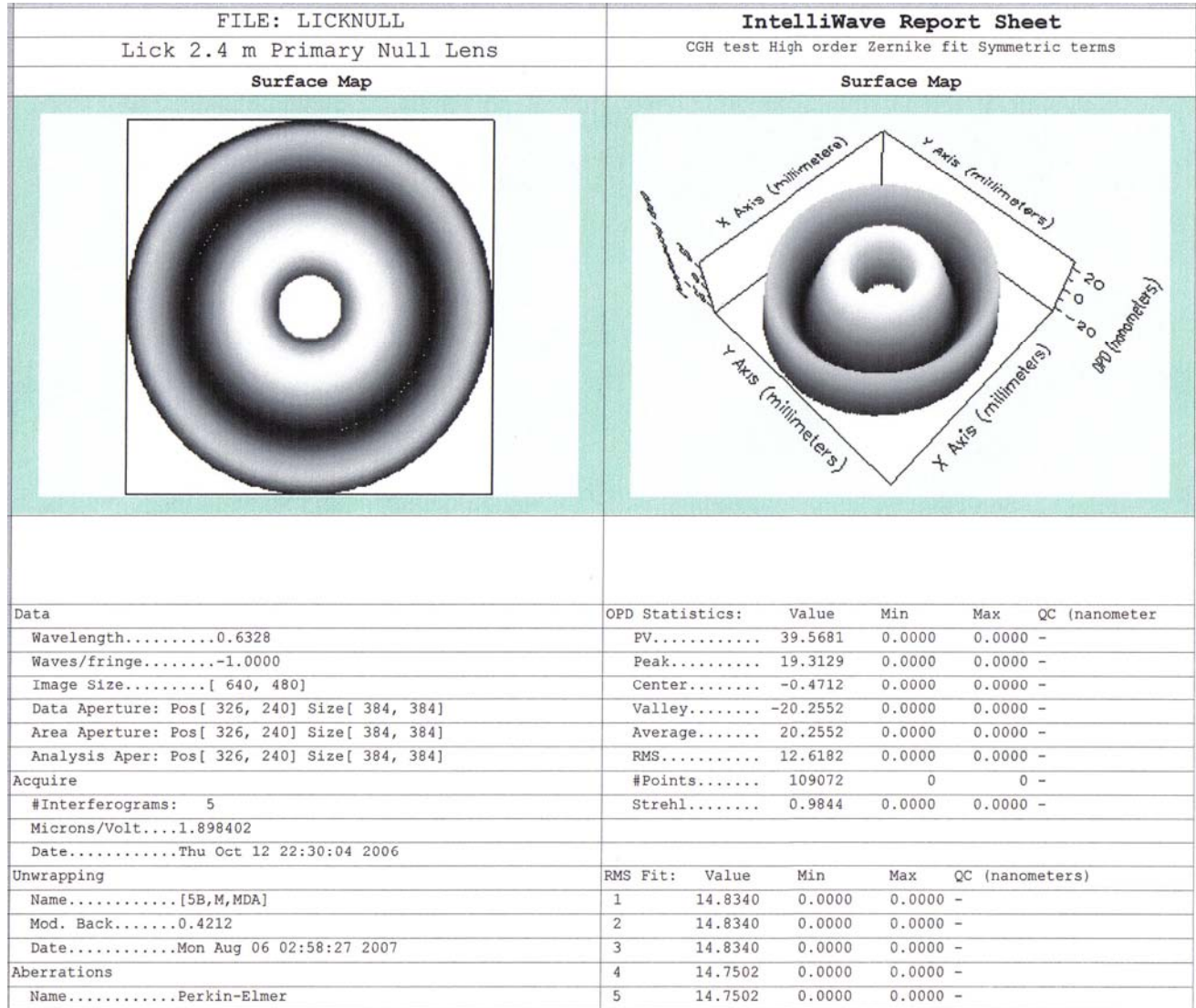


Figure 9a. The symmetric portion of the high-order Zernike fit to the CGH data.

Engineering Synthesis Design Inc. 6

	1				2			
23	Aperture Type...inscribed				6	14.7431	0.0000	0.0000 -
24	Removed.....2,3,4,5,6,7,8,9,10,12,13,14,15,16,17,18,19				7	14.7431	0.0000	0.0000 -
25					8	6.2024	0.0000	0.0000 -
26					9	6.2024	0.0000	0.0000 -
27	Aber>Perkin: Value	Min	Max	QC (nanometers)	10	2.9709	0.0000	0.0000 -
28	1) Piston:	-1.3349	0.0000	0.0000 Removed	11	2.9709	0.0000	0.0000 -
29	2) Tilt:	0.0000	0.0000	0.0000 Removed	12	2.5959	0.0000	0.0000 -
30	3) Tilt:	-0.0000	0.0000	0.0000 Removed	13	2.5959	0.0000	0.0000 -
31	4) Focus:	-0.1070	0.0000	0.0000 Removed	14	2.2068	0.0000	0.0000 -
32	5) Astig:	0.0000	0.0000	0.0000 Removed	15	2.2068	0.0000	0.0000 -
33	6) Astig:	-0.0000	0.0000	0.0000 Removed	16	1.6641	0.0000	0.0000 -
34	7) Coma:	0.0000	0.0000	0.0000 Removed	17	1.6641	0.0000	0.0000 -
35	8) Coma:	0.0000	0.0000	0.0000 Removed	18	0.0000	0.0000	0.0000 -
36	9) Coma:	-0.0000	0.0000	0.0000 Removed				
37	10) Coma:	-0.0000	0.0000	0.0000 Removed				
38	11) Spherical:	3.4804	0.0000	0.0000 -				
39	12) Astig:	0.0000	0.0000	0.0000 Removed				
40	13) Astig:	-0.0000	0.0000	0.0000 Removed				
41	14) Astig:	-0.0000	0.0000	0.0000 Removed				
42	15) Astig:	0.0000	0.0000	0.0000 Removed				
43	16) Coma:	0.0000	0.0000	0.0000 Removed				
44	17) Coma:	0.0000	0.0000	0.0000 Removed				
45	18) Coma:	0.0000	0.0000	0.0000 Removed				
46	19) Coma:	0.0000	0.0000	0.0000 Removed				
47	20) Coma:	0.0000	0.0000	0.0000 Removed				
48	21) Coma:	0.0000	0.0000	0.0000 Removed				
49	22) Spherical:	-1.2656	0.0000	0.0000 -				
50	23) Astig:	0.0000	0.0000	0.0000 Removed				
51	24) Astig:	-0.0000	0.0000	0.0000 Removed				
52	25) Astig:	-0.0000	0.0000	0.0000 Removed				
53	26) Astig:	0.0000	0.0000	0.0000 Removed				
54	27) Astig:	0.0000	0.0000	0.0000 Removed				
55	28) Astig:	-0.0000	0.0000	0.0000 Removed				
56	29) Coma:	0.0000	0.0000	0.0000 Removed				
57	30) Coma:	-0.0000	0.0000	0.0000 Removed				
58	31) Coma:	0.0000	0.0000	0.0000 Removed				
59	32) Coma:	-0.0000	0.0000	0.0000 Removed				
60	33) Coma:	-0.0000	0.0000	0.0000 Removed				
61	34) Coma:	0.0000	0.0000	0.0000 Removed				
62	35) Coma:	-0.0000	0.0000	0.0000 Removed				
63	36) Coma:	0.0000	0.0000	0.0000 Removed				
64	37) Spherical:	-40.1195	0.0000	0.0000 -				

Figure 9b. The first 50 coefficients of the high order Zernike fit where all asymmetric terms have been subtracted leaving only the symmetric errors

1.3. Test optic determination.

In addition to the radially symmetric errors measured with the CGH there are the non-rotationally symmetric (or asymmetric) errors which must be measured and added to the symmetric errors for a final determination of the test optic errors. As shown in the phase map above, the null corrector contains some asymmetric error as well as some error due to the misalignment of the corrector to the source point. These errors are combined with the errors found in the three fold flats that form the test optic errors. To determine the contributions of the null corrector and fold flats to the test optic asymmetric error we performed a set of measurements of the mirror at 4 rotational orientations 90 degrees apart. High order Zernike fits to each of the measurements are made and the 4 measurements are averaged. The asymmetric error terms of the mirror will average to zero leaving just contributions from the test optics that do not rotate from test to test. There will still remain some small amount of local asymmetric error not fit by the Zernikes but that will be averaged down by a factor of 4 when the maps are finally derotated and averaged together to give the final measurement of the mirror after subtraction of the measured test optics. Since the test optics are very smooth surfaces and the fit is to high order (205 terms) we can assume that the test optic errors will be well fit by the Zernike polynomials. This is certainly evidenced in the CGH test of the null corrector shown above and independent measures of the fold flats show them to be very smooth surfaces.

To accurately remove these errors from the test data the Zernike fit data is used for several reasons:

1. The CGH and rotation data contains a small high frequency component which is effectively smoothed out by the Zernike fit.
2. Since the Zernike polynomial representation of the test optics is independent of the magnification or position of the image in the actual test it simplifies the subtraction of the errors by not requiring accurate alignment of the test optic phase data and mirror phase data.

Since this is a focal system power errors in the flats do not contribute to the test optic errors except in the case of fold flat 3 which, used at 45 degrees, will show some astigmatism with power error in its surface due to the non-normal angle of incidence. These errors, however, are well fit by the Zernike polynomials. Non-power symmetric errors in the flats, although very small, form the main contribution to the uncertainty in the measurement since they cannot be measured by the mirror rotations. These errors are given in the Appendix in the Test Plan.

Shown in the next series of 4 figures, Figures 10-13, are the results from each of the rotation tests. The Zernike polynomials are from a low order 36 term fit done for the purposes of identifying tilt, focus, and coma terms which were subtracted from each measurement. All units are in nanometers.

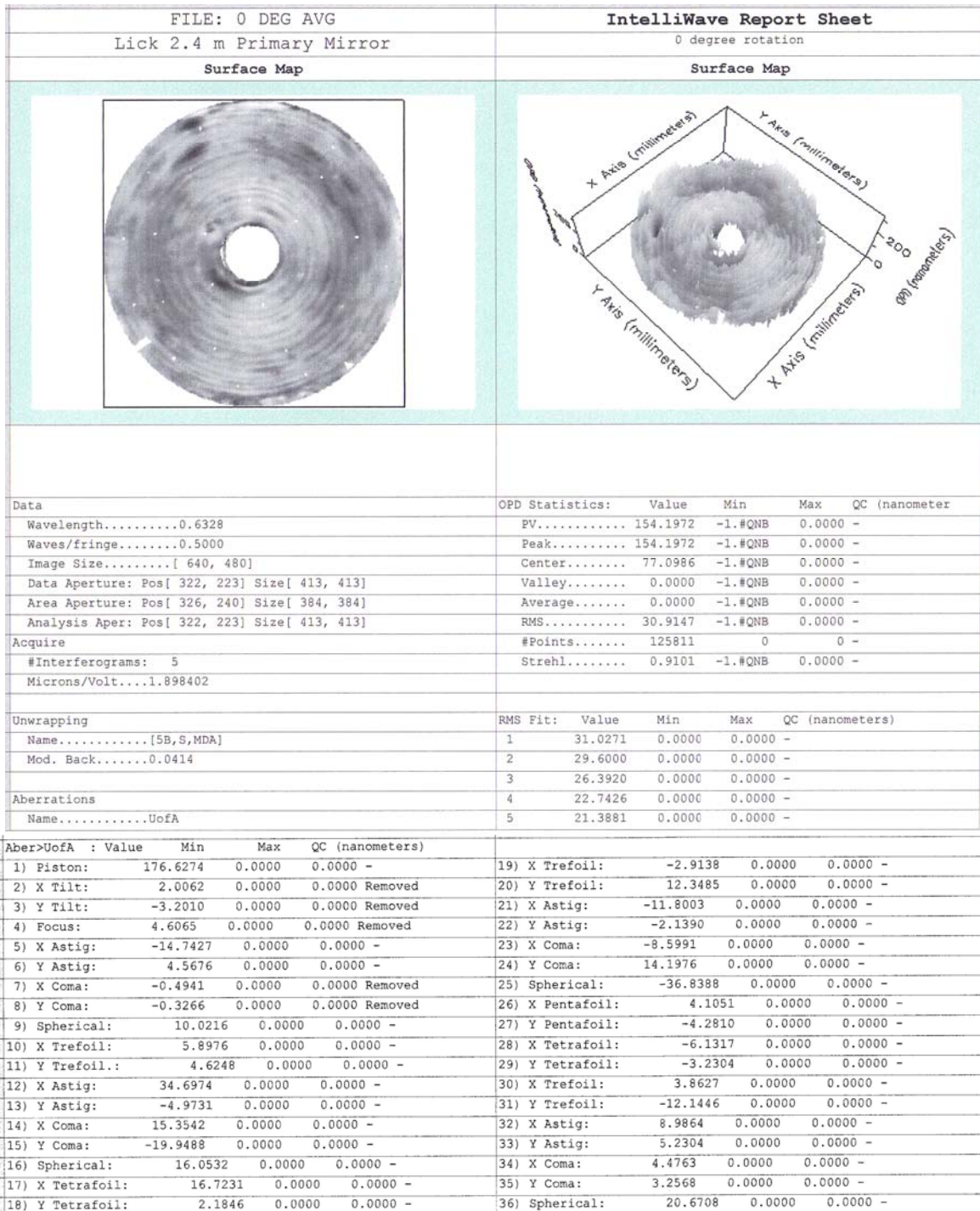


Figure 10. A surface map of the mirror tested at the 0 degree position. The coefficients are those to a 36 term (UofA) set of Zernike polynomials.

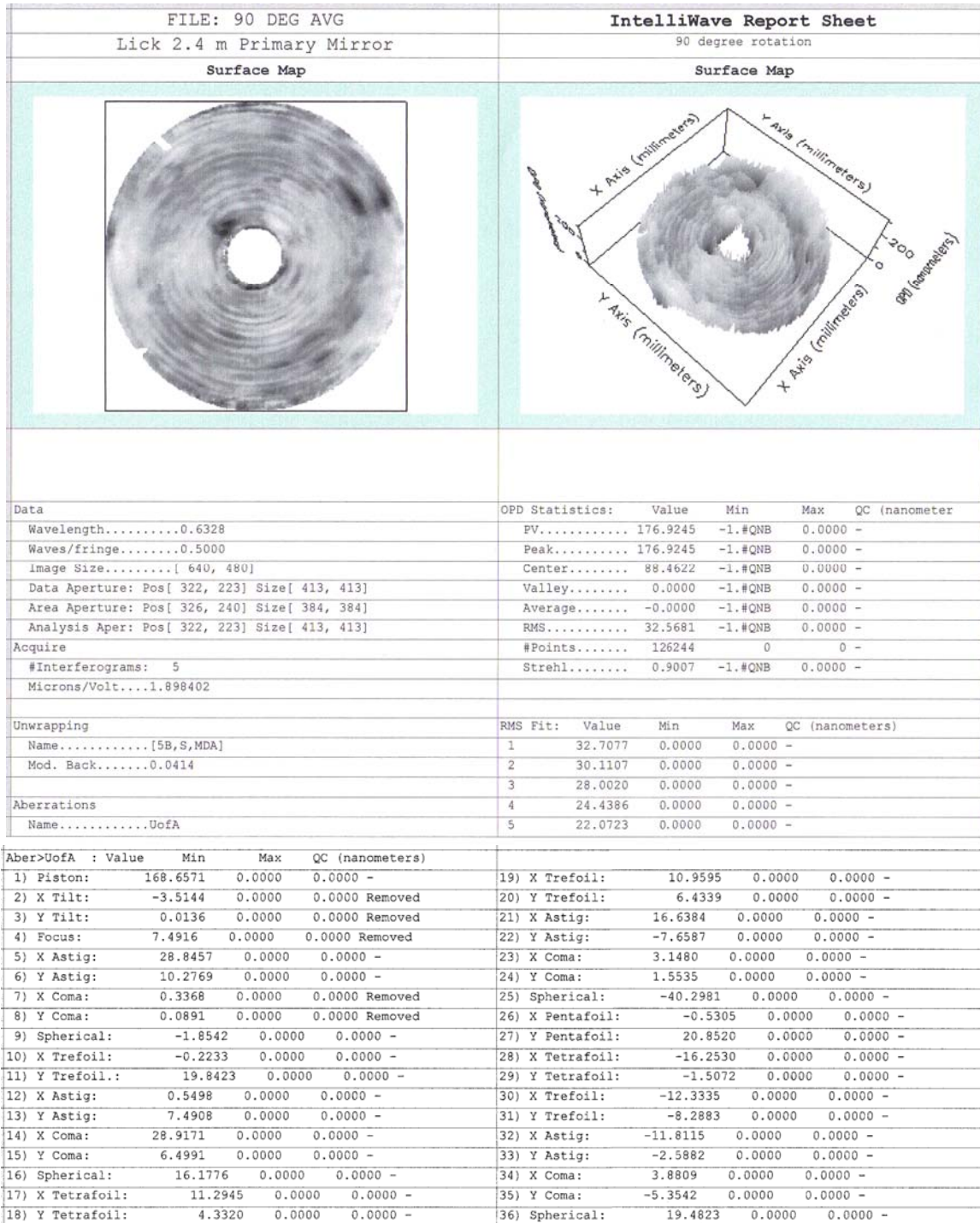


Figure 11. The phase map and Zernike polynomial coefficients of the mirror rotated 90 degrees.

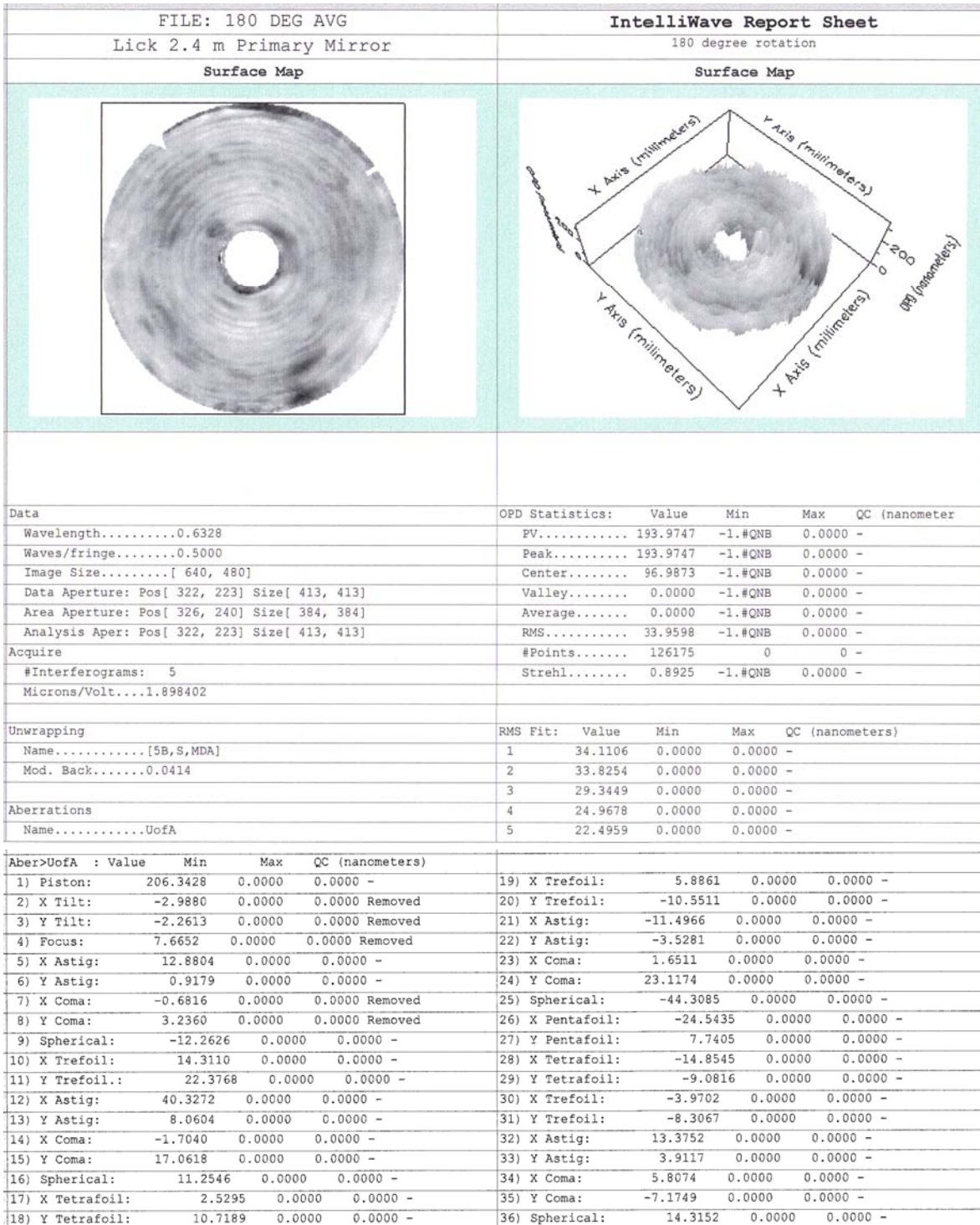


Figure 12. The phase map and Zernike polynomial coefficients of the mirror rotated 180 degrees.

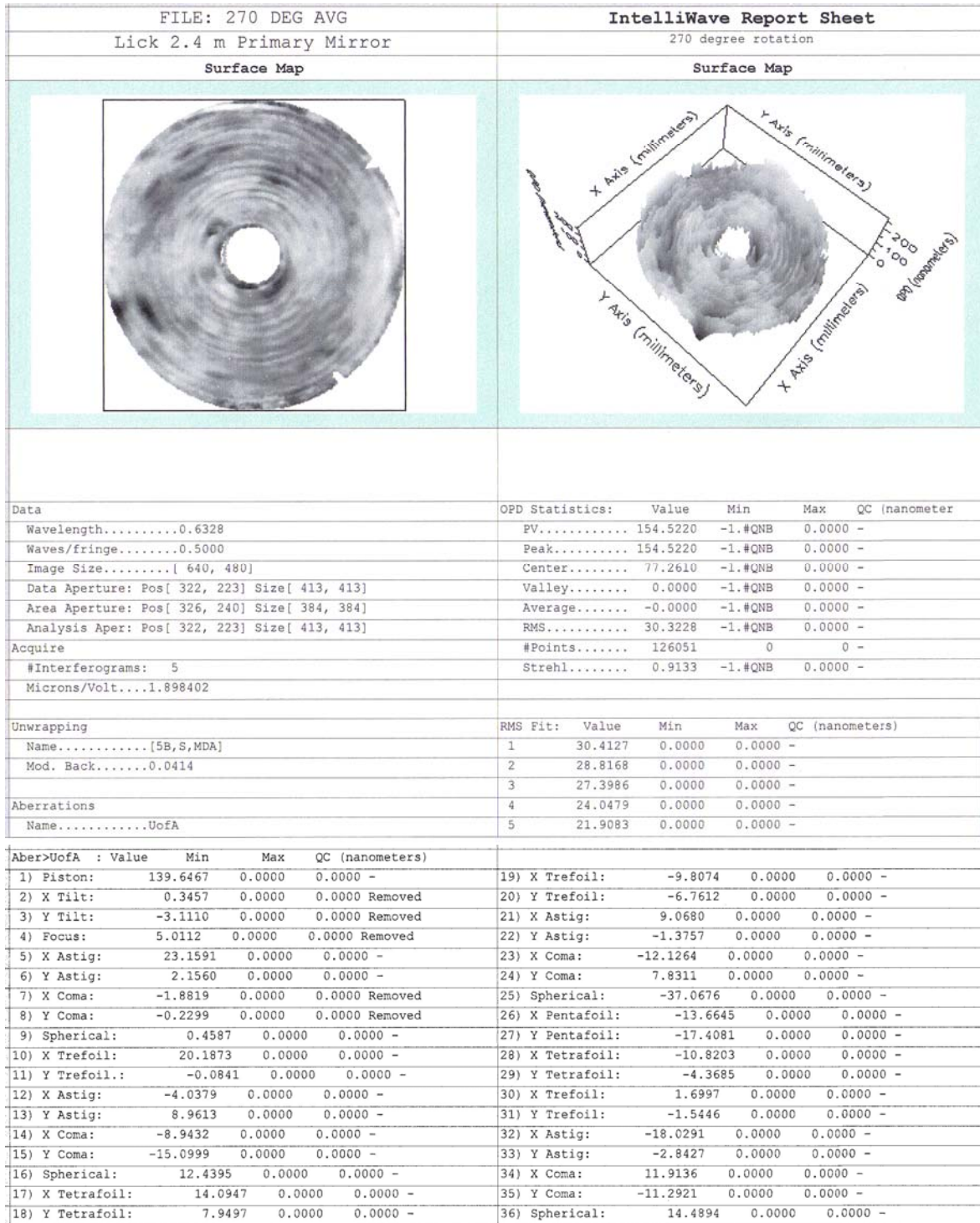


Figure 13. The phase map and Zernike polynomial coefficients for the mirror rotated 270 degrees.

These four rotation maps were averaged to average out the Zernike polynomials except for the tetrafoil terms. The average map is shown in Figure 14. A high order Zernike fit is made to this map and the symmetric terms are subtracted along with the tetrafoil terms since they are all indeterminate from this average. The complete list of the high order Zernike coefficients can be found in the Appendix. Shown in Figure 15 is a map of the high order Zernike terms that form the asymmetric part of the test optics. This map is then added to the symmetric terms of the CGH test of the null corrector that forms the completed map of the test optics shown in Figure 16a that is subtracted from the mirror tests. An interferogram produced from the test optics phase map is shown in Figure 16b.

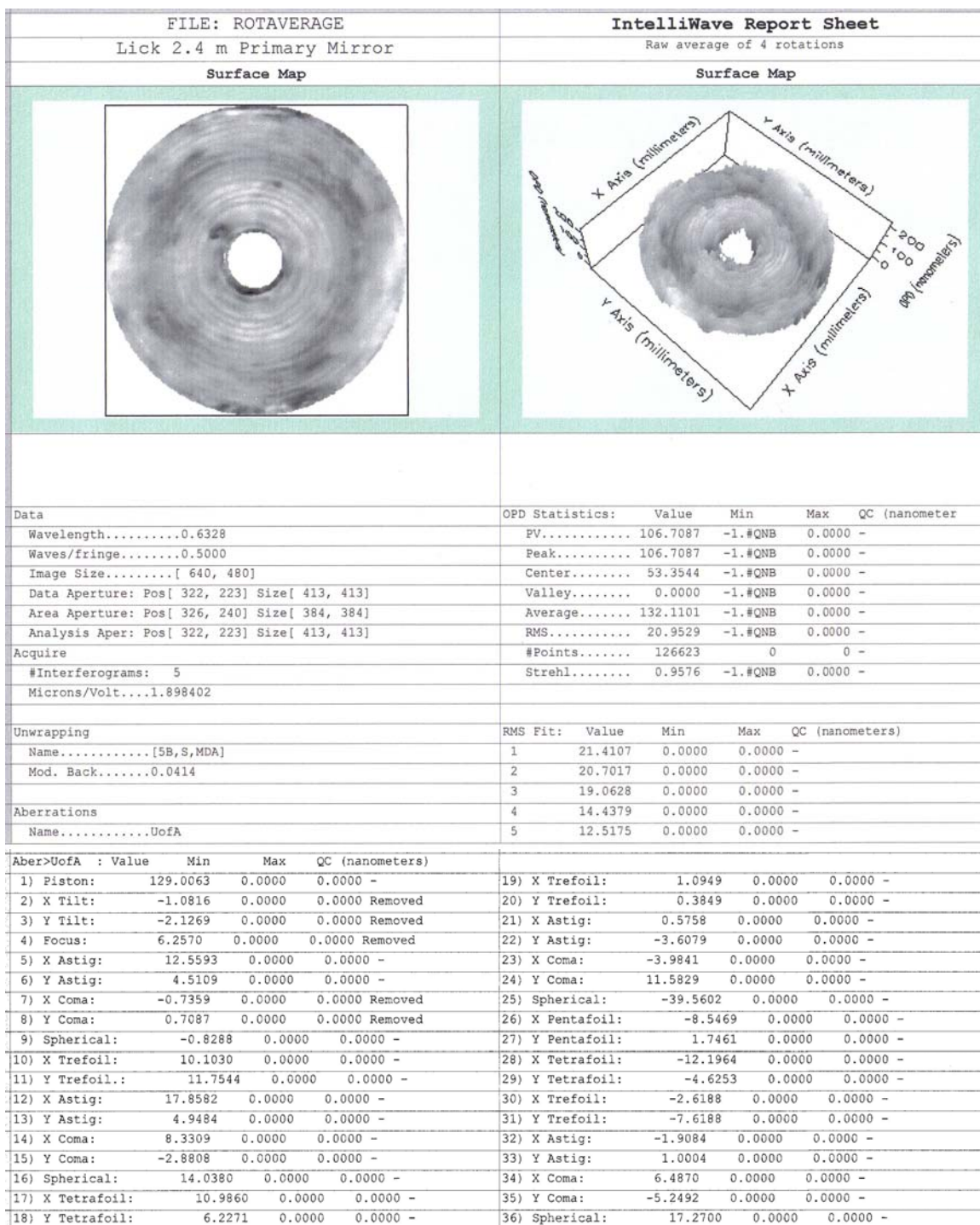


Figure 14. The average of the 4 rotations 90 degrees apart. The complete list of the high order Zernike terms can be found in the Appendix.

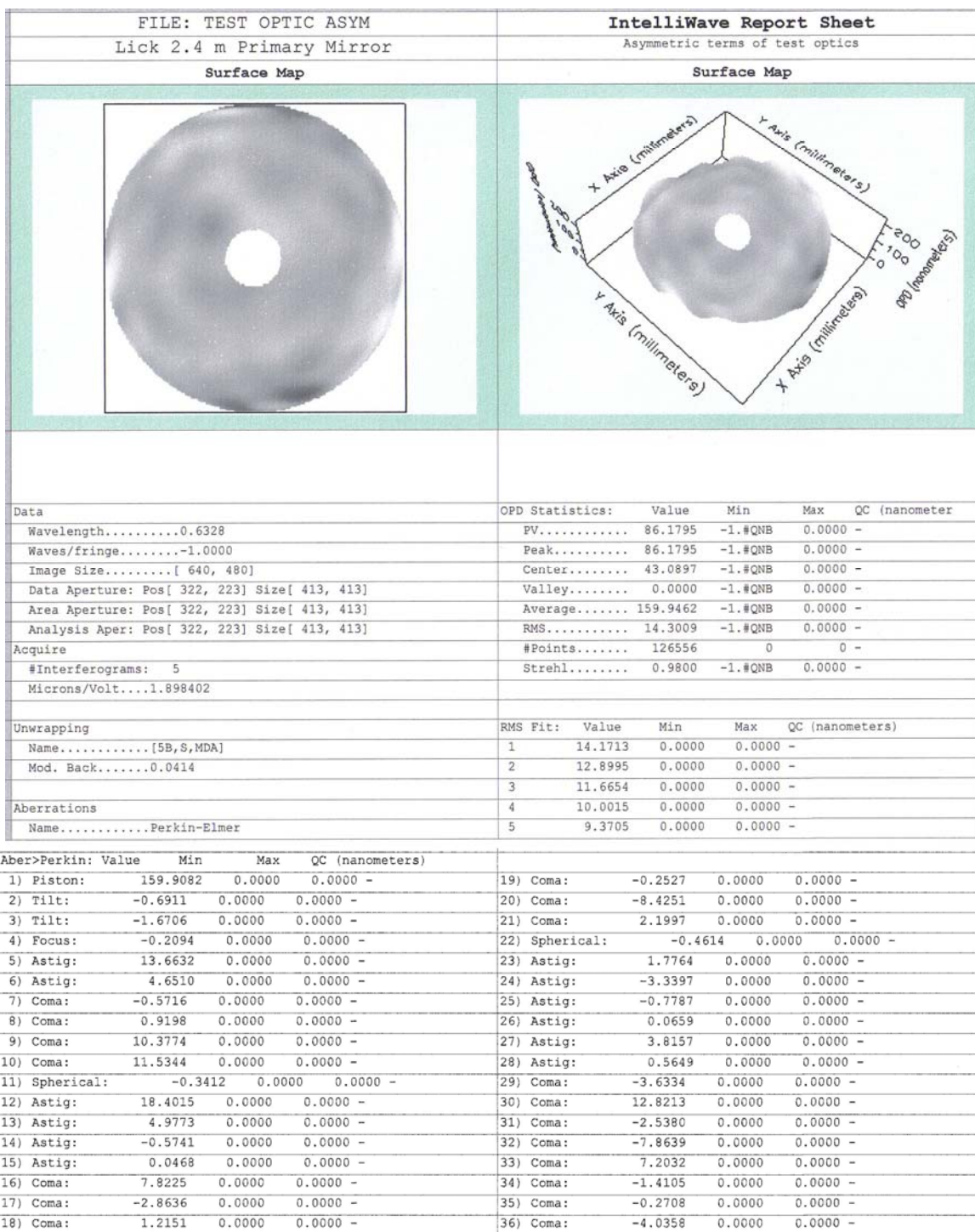


Figure 15. A phase map of the asymmetric terms of the test optics. The first 36 terms are shown here with a complete listing found in the Appendix.

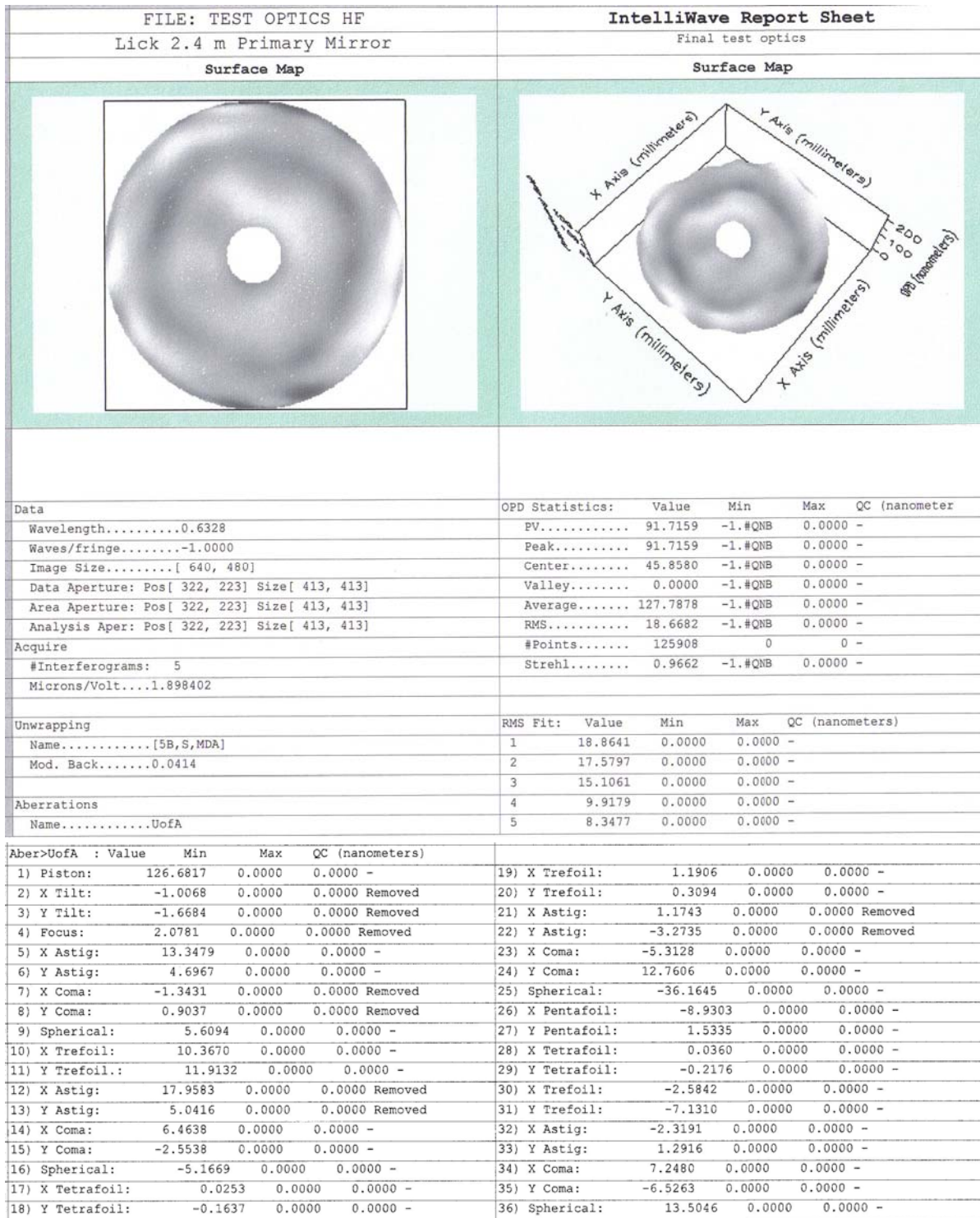


Figure 16a. A map of the test optics that is subtracted from the test data.

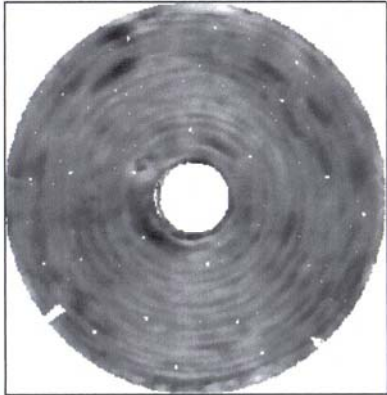
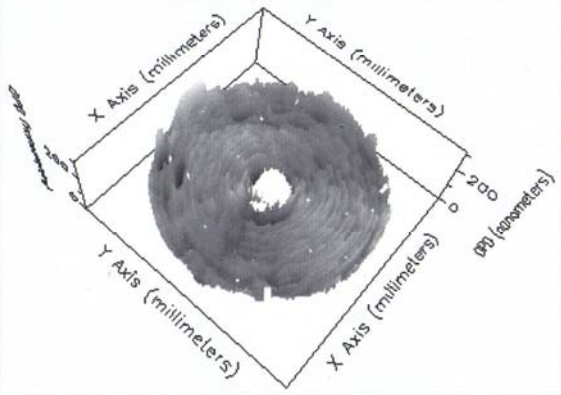
Interferogram #2



Figure 16b. An interferogram produced from the final test optics phase map.

1.4. Final figure of the mirror.

The test optics map from Figure 16 is subtracted from each of the raw measurements taken at each of the 4 rotation positions. The resulting maps are shown in Figures 17-20. These maps are then derotated to all be in the same orientation as the 0 degree position and averaged. This average is the best estimate map of the mirror's figure having a rms surface error of 23.6 nm. When this is RSS summed with the estimated uncertainties given in the Test Plan yields a final surface figure value of 24.7 nm rms. This value multiplied by two gives a wavefront error of 49.4 nm rms.

FILE: 0 DEG AVG MINUS REF Lick 2.4 m Primary Mirror		IntelliWave Report Sheet 0 degree test minus test optics			
Surface Map		Surface Map			
					
Data	OPD Statistics:	Value	Min	Max	QC (nanometer)
Wavelength.....0.6328	PV.....	136.0607	-1.#QNB	0.0000	-
Waves/fringe.....0.5000	Peak.....	136.0607	-1.#QNB	0.0000	-
Image Size.....[640, 480]	Center.....	68.0304	-1.#QNB	0.0000	-
Data Aperture: Pos[322, 223] Size[413, 413]	Valley.....	0.0000	-1.#QNB	0.0000	-
Area Aperture: Pos[326, 240] Size[384, 384]	Average.....	133.1628	-1.#QNB	0.0000	-
Analysis Aper: Pos[322, 223] Size[413, 413]	RMS.....	27.1003	-1.#QNB	0.0000	-
Acquire	#Points.....	125172	0	0	-
#Interferograms: 5	Strehl.....	0.9302	-1.#QNB	0.0000	-
Microns/Volt....1.898402					
Unwrapping	RMS Fit:	Value	Min	Max	QC (nanometers)
Name.....[5B,S,MDA]	1	27.1529	0.0000	0.0000	-
Mod. Back.....0.0414	2	24.4892	0.0000	0.0000	-
	3	21.5265	0.0000	0.0000	-
Aberrations	4	20.1468	0.0000	0.0000	-
Name.....UofA	5	19.0743	0.0000	0.0000	-

Aber>UofA	: Value	Min	Max	QC (nanometers)				
1) Piston:	132.1052	0.0000	0.0000	0.0000 -	19) X Trefoil:	-4.7273	0.0000	0.0000 -
2) X Tilt:	2.7138	0.0000	0.0000	Removed	20) Y Trefoil:	12.2506	0.0000	0.0000 -
3) Y Tilt:	-0.8820	0.0000	0.0000	Removed	21) X Astig:	-13.3777	0.0000	0.0000 -
4) Focus:	3.8179	0.0000	0.0000	Removed	22) Y Astig:	0.8962	0.0000	0.0000 -
5) X Astig:	-27.4641	0.0000	0.0000	-	23) X Coma:	-2.4914	0.0000	0.0000 -
6) Y Astig:	-0.2162	0.0000	0.0000	-	24) Y Coma:	1.1858	0.0000	0.0000 -
7) X Coma:	1.2269	0.0000	0.0000	Removed	25) Spherical:	-2.1079	0.0000	0.0000 -
8) Y Coma:	-2.0112	0.0000	0.0000	Removed	26) X Pentafoil:	13.3979	0.0000	0.0000 -
9) Spherical:	2.8935	0.0000	0.0000	-	27) Y Pentafoil:	-6.3577	0.0000	0.0000 -
10) X Trefoil:	-4.6351	0.0000	0.0000	-	28) X Tetrafoil:	-5.9041	0.0000	0.0000 -
11) Y Trefoil.:	-6.7394	0.0000	0.0000	-	29) Y Tetrafoil:	-3.0935	0.0000	0.0000 -
12) X Astig:	16.5764	0.0000	0.0000	-	30) X Trefoil:	5.7296	0.0000	0.0000 -
13) Y Astig:	-10.3652	0.0000	0.0000	-	31) Y Trefoil:	-4.3583	0.0000	0.0000 -
14) X Coma:	9.4695	0.0000	0.0000	-	32) X Astig:	10.0229	0.0000	0.0000 -
15) Y Coma:	-18.3702	0.0000	0.0000	-	33) Y Astig:	3.5717	0.0000	0.0000 -
16) Spherical:	23.7598	0.0000	0.0000	-	34) X Coma:	-2.0241	0.0000	0.0000 -
17) X Tetrafoil:	16.4508	0.0000	0.0000	-	35) Y Coma:	7.9501	0.0000	0.0000 -
18) Y Tetrafoil:	2.4405	0.0000	0.0000	-	36) Spherical:	10.3616	0.0000	0.0000 -

Figure 17. Test at 0 degrees minus the test optics

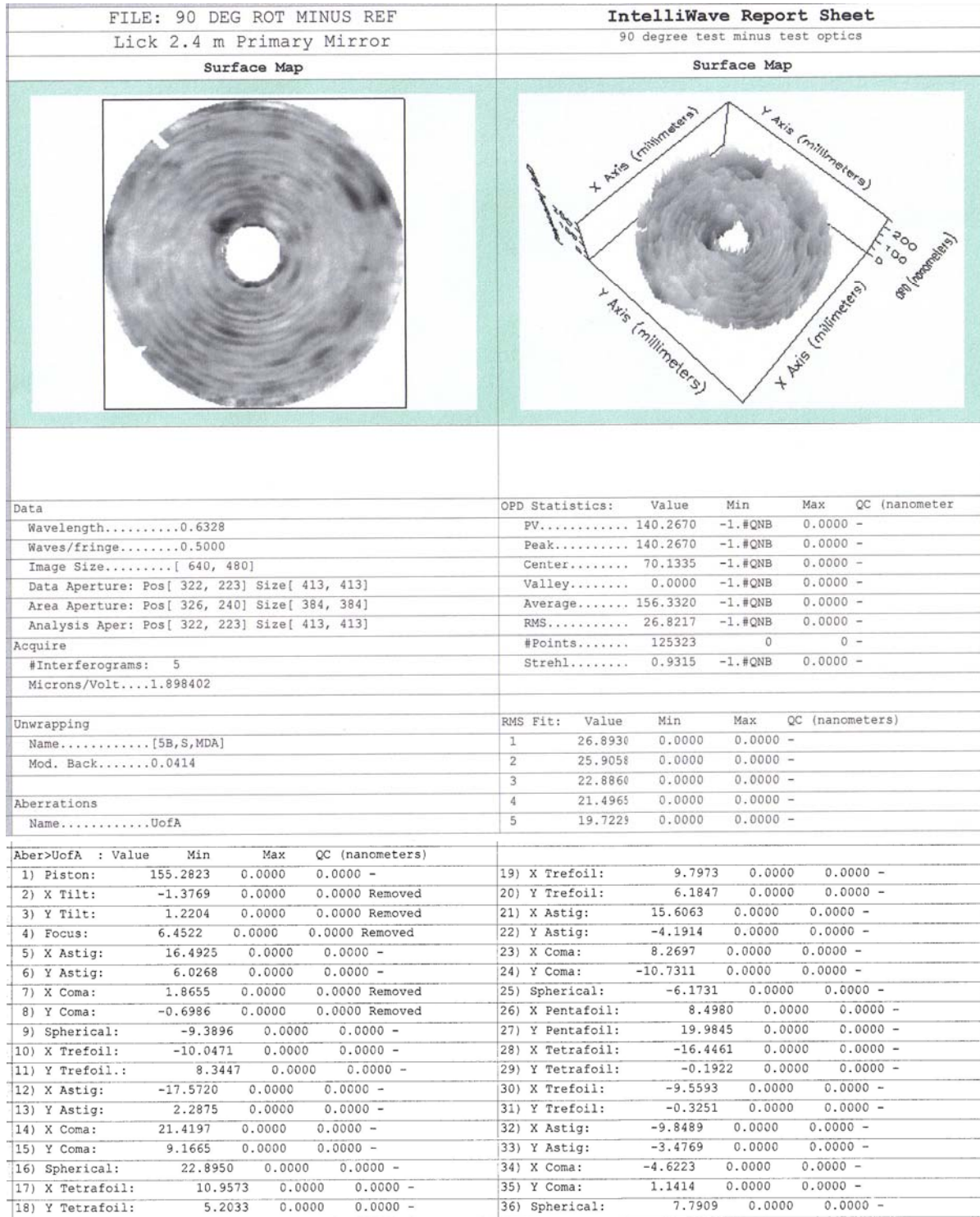


Figure 18. 90 degree position test minus test optics.

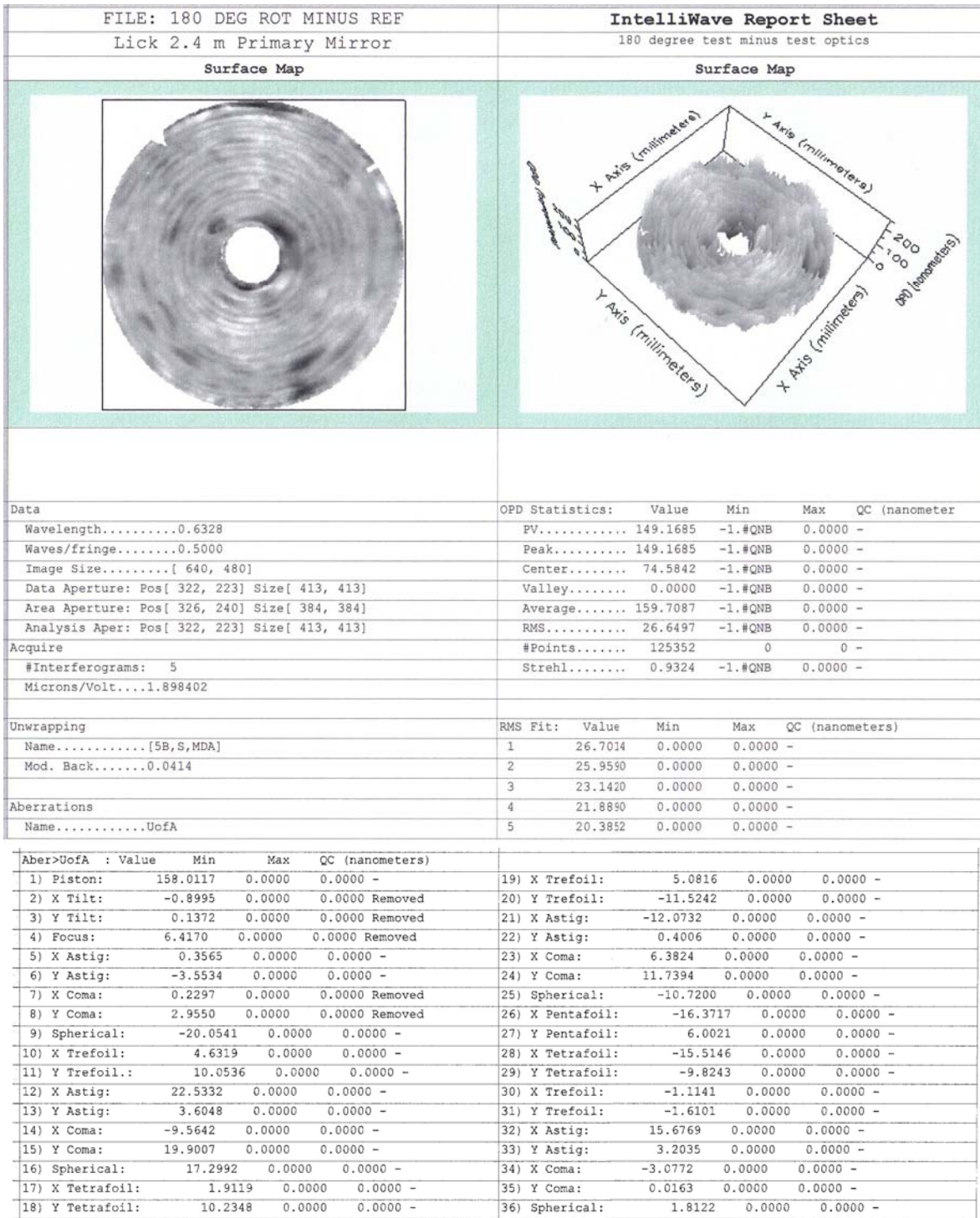


Figure 19. 180 degree test minus test optics.

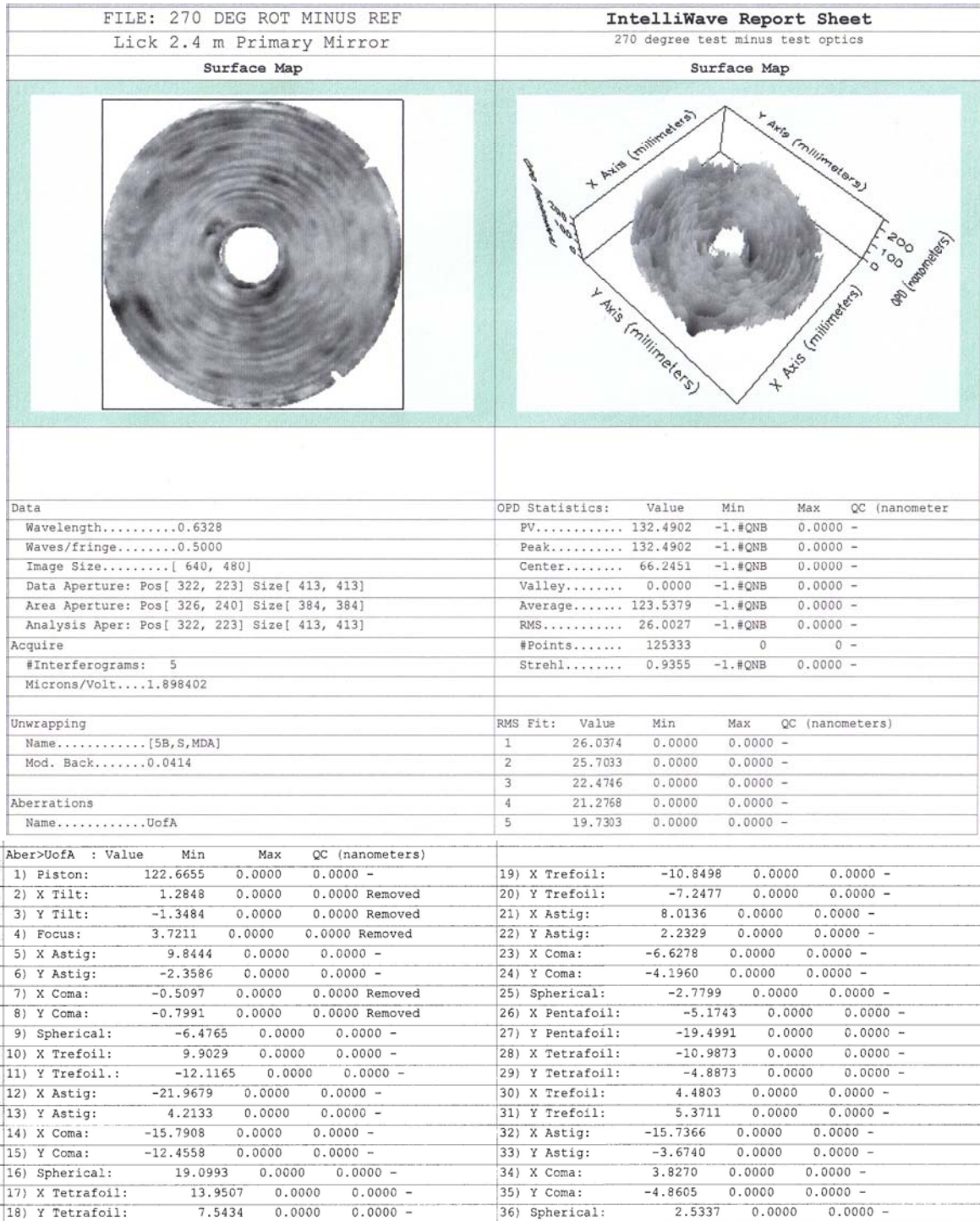


Figure 20. 270 degree position test minus test optics.

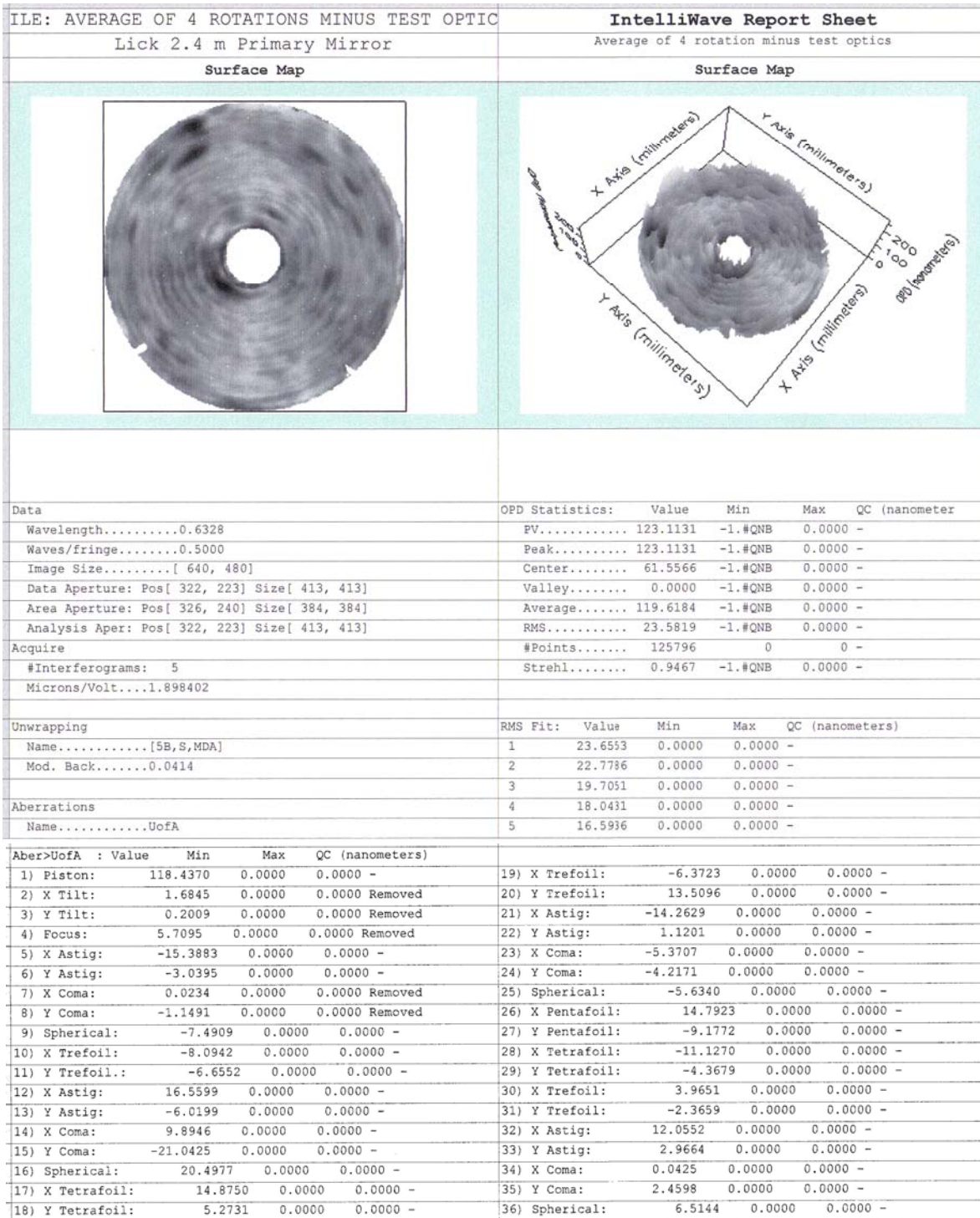


Figure 21. The final phase map and Zernike coefficients produced from the average of the 4 derotated test position measurements.

1.5. Centration of the optical axis.

Decentration of the optical axis results in an asymmetrical surface with the error being principally coma. To measure the magnitude and direction of the decentration we need to measure the amount and direction of the coma in the mirror's surface. Because there is also coma produced by a misalignment of the null corrector with respect to the mirror's axis during an optical test that error must be separated from the actual coma in the mirror in order to correctly measure the decentration.

In the original test plan a method is described to measure the coma by first nulling the fringes at one rotational position then rotating the mirror by 180° and measuring the coma observed. In that plan the coma is presumed to be small so that the Intellwave software can be used. Because the mirror is so fast a small amount of coma results in a large amount of coma in the test. We found that upon rotation there was significant coma that precluded phase measurement of the coma. Instead we have used the test design shown in Figure 4 to model the test in ZEMAX and measure the coma by counting fringes in the interferogram.

The specification for the mirror is for the decentration to be less than 2 mm. Figure 22 is an interferogram produced by ZEMAX for what the interferometer would show upon the 180° rotation from an initial nulled position if the mirror had a full 2mm of decentration. Note that this is exactly twice the amount of coma that would be in the mirror's surface since the aberrated mirror was initially nulled at the 0° position by balancing the coma in the mirror with the coma from a null corrector misalignment. The total P-V coma in the interferogram of 38.8 waves is due to 19.4 waves of coma in the surface for the 2 mm decenter of the axis.

To perform the test, 4 indicators are mounted from the tower to the mirror in pairs 90° apart, one indicator of each pair measuring decenter and the other tilt. The mirror is positioned at the 0 degree position and the indicators are all zeroed. The fringes are then nulled and the mirror rotated 180° . Adjustment screws were added to the tower to be able to move the mirror and its cell in both tilt and decenter so that the mirror's surface could be positioned so that the indicators again all read zero. The amount of surface coma now observed in the test is twice that in the mirror's surface. Figure 23 is an interferogram taken at the rotated position.

Counting fringes in the interferogram we find that there are 24 waves of surface coma (48 fringes) in the test. This implies there are 12 waves of coma in the surface corresponding to 1.2 mm of decenter of the optical axis from its mechanical center defined by the outer edge of the mirror where the indicators were located.

The direction of the decenter is found from the direction of the coma. The direction of the decenter will be in the direction of the high edge of the coma. From the interferogram, the high edge of the coma is located approximately 72° clockwise from the Top fiducial.

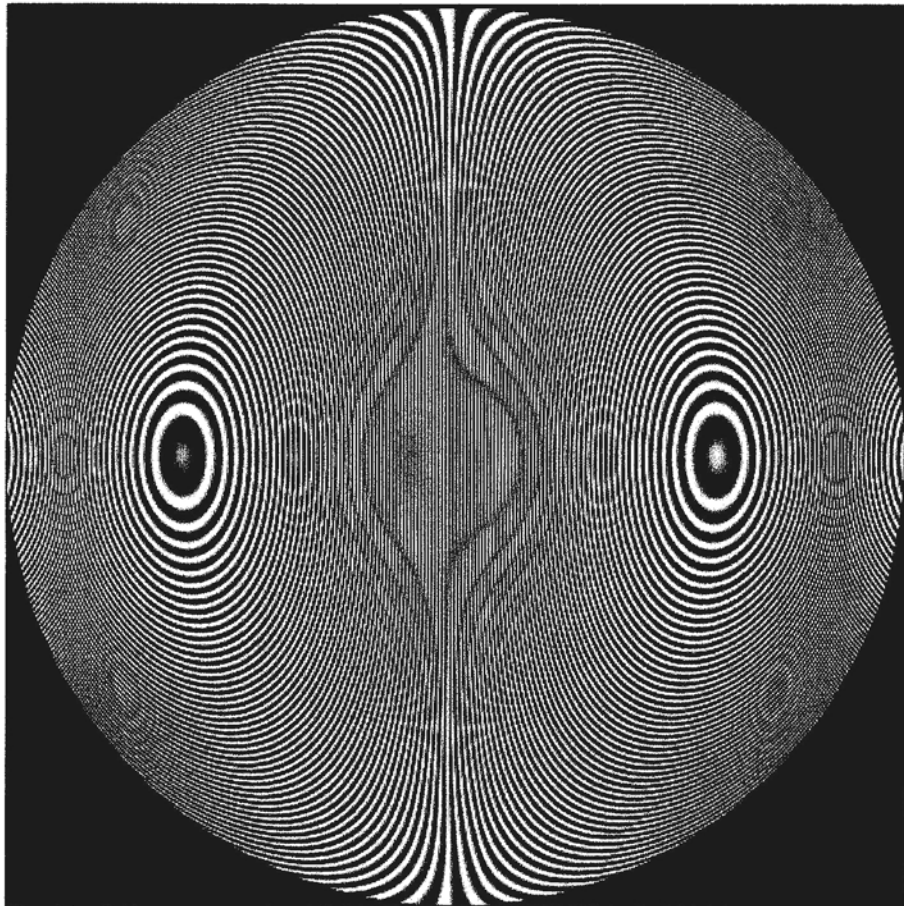


Figure 22. An interferogram of the coma of the primary mirror decentered in the X direction by 2 mm after rotation of 180° from a nulled position.

Interferogram #1

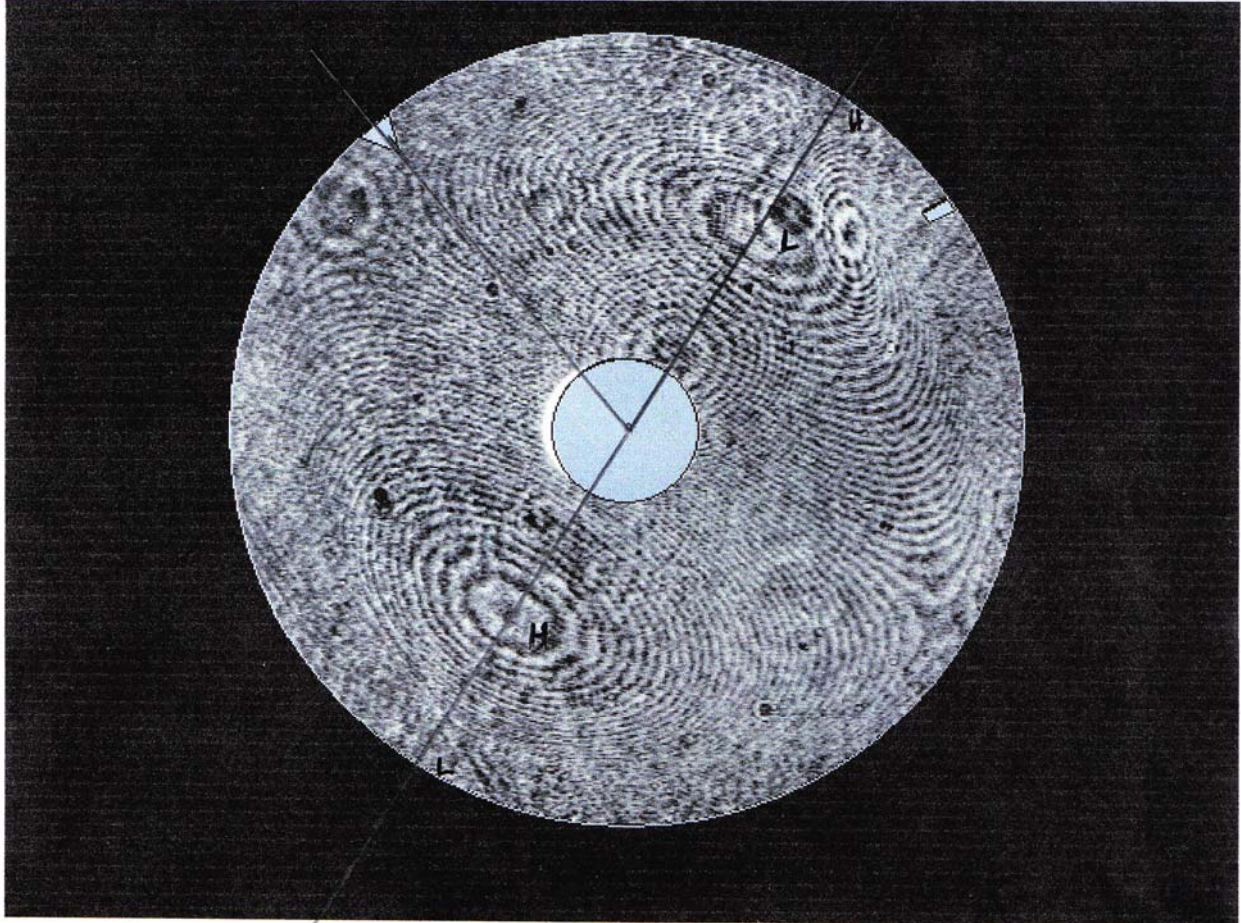


Figure 23. An interferogram of the mirror rotated through 180° from an initial null at the 0° position. The coma is twice that due to the mirror's decenter. The direction of the coma determines the direction of the decenter.

2. Radius of Curvature and Conic Constant.

2.1. Measurement of the radius of curvature.

Referring to the description of the measurement of the radius of curvature in the Test Plan included in the Appendix the radius measurement involves measuring three distances, the distance from fold flat three to the mirror, and the distances between fold flats 3 and 2 and between 2 and 1 whose surface lies at the paraxial center of curvature. The following distances were measured following the completion of figuring:

$$D_1 = 6715 \text{ mm}$$

$$D_2 = 372.5 \text{ mm}$$

$$D_3 = 119.4 \text{ mm}$$

The paraxial radius of curvature = $D_1 + D_2 + D_3 = 7206.9 \text{ mm}$.

2.2 Measurement of the conic constant.

The computer-generated hologram (CGH) used in the verification of the null corrector provides an independent verification of the conic constant as well as an easy means of determining the asymmetric errors in the corrector. In this test the CGH appears to the null corrector to be a full-sized primary mirror having the correct surface shape. The CGH will produce a null test when the null corrector is properly configured for the design radius of curvature and conic constant. If the radius of curvature of the mirror differs from the design radius of curvature of the CGH and null corrector then if the test of the mirror produces a null test the conic constant will differ from the design value given by the relation:

$$\Delta K / K = -\Delta R / R$$

The measured radius of curvature of the mirror is 7206.9 mm. This is different from the design radius of 7200 mm by 6.9 mm. This difference produces a change in the conic constant of .00096 or a conic constant of $K = -.99904$.

The other contribution to the conic constant is the residual spherical aberration measured in the final test. From the Zernike fit in Figure 21 the mirror was measured to have -7.5 nm of third order Zernike spherical aberration. This is equal to a P-V spherical aberration of -11.25 nm

meaning the mirror is slightly overcorrected. This is equivalent to a change in conic constant of $\Delta = -.000065$. The sum of this change and that of the radius change gives the final conic constant to be $K = -0.9991$.

3. Cosmetic Quality.

3.1. Scratch/Dig

Inspection of the surface was performed using bright illumination and the defects were mapped as shown in Figure 24. No scratches within the clear aperture were out of specification. There were numerous bubbles in the surface that exceed the dig specification and these are shown in the map. One inclusion at about 5:00 from the top fiducial was ground out during the fabrication as it was the source of continual tearing (crowfeet) of the surface resulting in a 2mm diameter dig in the surface. There are also some scratches outside the clear aperture at both the outside edge and inside edge that are not shown on the map.

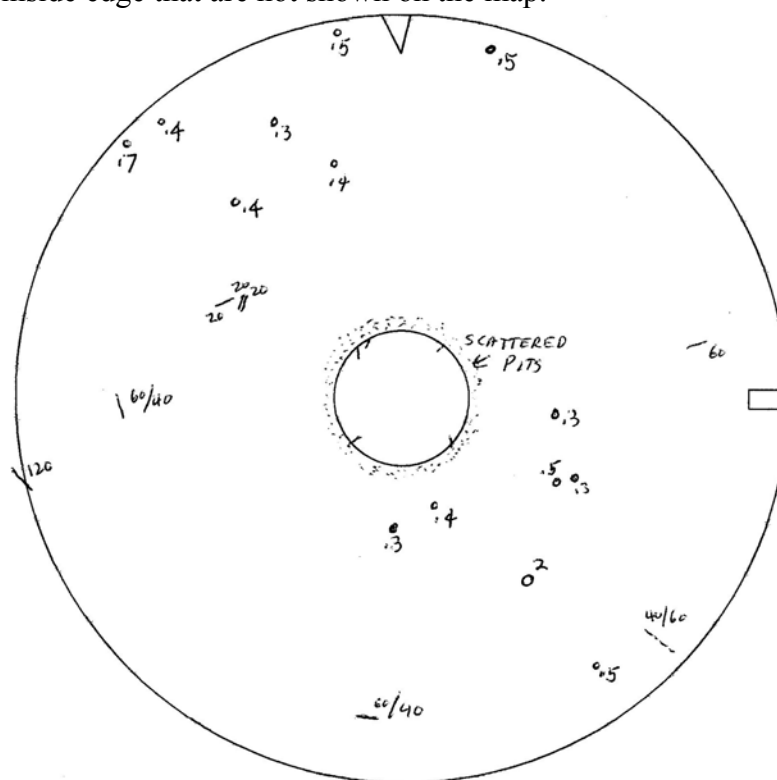


Figure 25. A map of the surface showing the locations of scratches and digs. The scratch widths are in microns and the dig diameters are in millimeters. There is some scattered pitting around the center hole extending out approximately 50 mm.

3.2. Surface microroughness.

Due to the very large backscatter from the Astro-Sital material a wedge shaped segment of the mirror was coated with silver so that scattering measurements of the surface could be made with the portable Schmitt Systems scatterometer. Measurements of the surface roughness were made at 7 locations along this strip from center to edge and the results are shown in Figure 26 and Table 3. The mirror has a very good roughness structure except near the center hole. We found that the scattering increased dramatically within about 50 mm of the edge of the center hole. Upon inspecting the surface with a microscope we found that the surface near the center hole was still slightly “gray”, i.e., it has scattered pits left over from the aspherizing of the mirror. This had not been observed earlier due to the large backscatter from the material. This area did not see as much polishing as the rest of the surface because of the large amount of figuring we performed on the outer portion of the mirror to bring up a rolled edge.

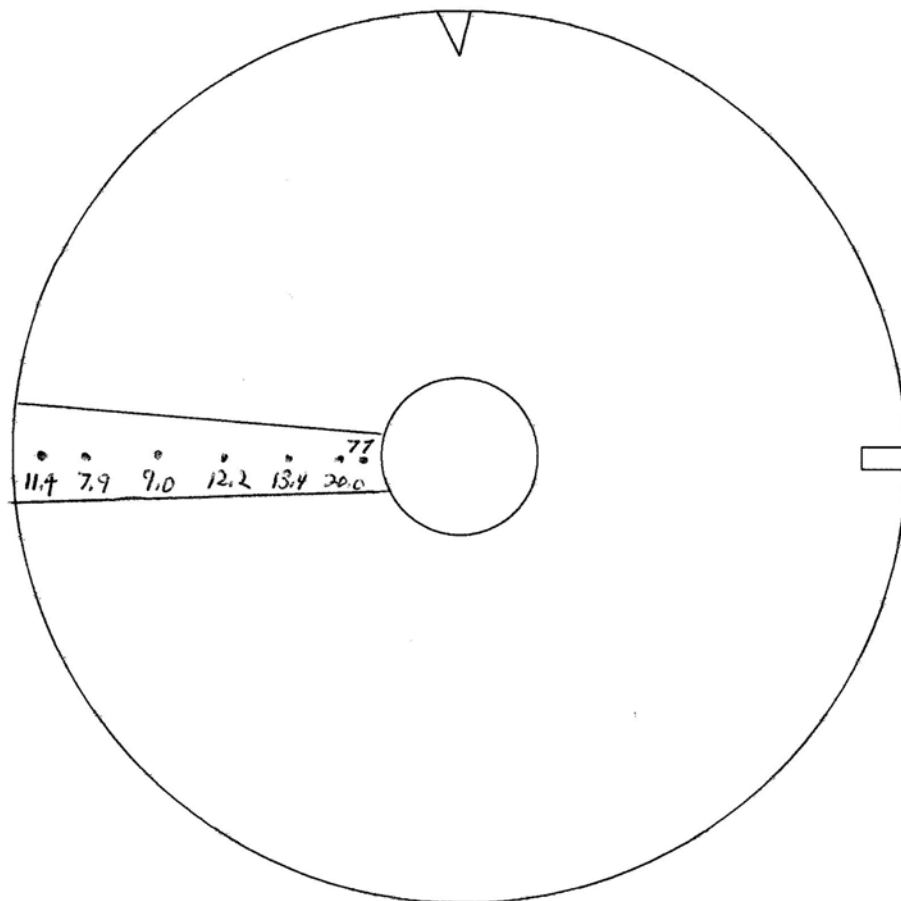


Figure 26. Surface roughness measurements across a radial segment. All measurements were within specification except for with 50 mm of the center hole where the scattering was measured at 77 angstroms rms.

Radial Position from Center (mm)	Roughness (angstroms rms)
180	77
300	20.0
440	13.4
570	12.2
840	9.0
1070	7.9
1150	11.4

Table 3. Scatterometer measurements as a function of radial distance from the center of the mirror.